# We are IntechOpen, the world's leading publisher of Open Access books Built by scientists, for scientists

**4,800**
Open access books available

**122,000**
International authors and editors

**135M**
Downloads

Our authors are among the

**154**
Countries delivered to

**TOP 1%**
most cited scientists

**12.2%**
Contributors from top 500 universities

CLARIVATE ANALYTICS BOOK CITATION INDEX INDEXED

WEB OF SCIENCE™

Selection of our books indexed in the Book Citation Index in Web of Science™ Core Collection (BKCI)

## Interested in publishing with us?
## Contact book.department@intechopen.com

Numbers displayed above are based on latest data collected.
For more information visit www.intechopen.com

# 9

# Single-Point Methods for Location of Distortion, Unbalance, Voltage Fluctuation and Dips Sources in a Power System

Zbigniew Hanzelka, Piotr Słupski, Krzysztof Piątek,
Jurij Warecki and Maciej Zieliński
*AGH-University of Science & Technology, Krakow*
*Poland*

## 1. Introduction

The old model in which the problem of power quality (PQ) involved two partners – the electricity supplier and the customer – is replaced by a new configuration where at least four, mutually dependent parties participate: the customer, supplier of electric power, manufacturer of equipment and electrical installation contractor. The supplier often insists that sources of disturbances are located at the customer's side, whereas the latter complains about causes located in the supply network. It happens that their discussion leads to the conclusion, shared by both parties, that the equipment is not properly installed or adequately designed, to be operated in the given electromagnetic environment.
Often, in the case of a significant level of a disturbance in electrical power system, at the customer's supply terminals, there is a need for locating the source of harmonics (e.g. [7-9,14,21,27,32-35,38,40-43]), voltage fluctuations (e.g. [10-13,36,]), voltage dips (e.g. [17,19,22,25,26,29-31,37,39]), occasionally also asymmetry. With the deregulation of power industry, utilities have become increasingly interested in quantifying the responsibilities for power quality problems. This issue gains particular meaning when formulating contracts for electric power supply and enforcing, by means of tariff rates, extra charges for worsening the power quality.

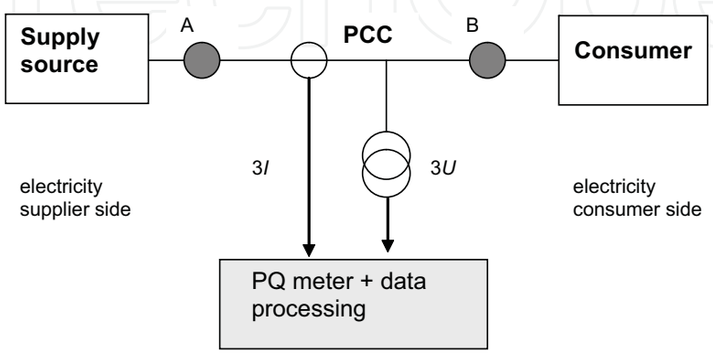


Fig. 1. Problem of locating the voltage disturbance sources

There are two, sometimes separate problems which can be stated as follows (Fig. 1). First details concerning the location of disturbance source. A power quality monitor captures disturbance-containing voltage and current waveforms at the point of common coupling (PCC). It is required to determine if the disturbance comes from the upstream or the downstream. As a result, both the supply utility and customer can obtain a list of disturbances, their severity and directions. Such information will greatly facilitate the resolution of disputes between the two parties if a disturbance results in financial losses to either party.
The second is to assess the emission level of the particular considered load or supplier in order to quantitative evaluation of the both parts contribution to the total disturbance level measured at the point of power delivery. The goal is to check the fulfilment of standard or contract requirements.
Solution for both problems posed above is not a trivial task. Works focused on this subject have been carried out for many years. Numerous methods have been proposed and published, only a part of them having practical significance. They differ in the probability of inference correctness (e.g. locating a disturbance source), the value of error made (e.g. determining an individual customer's share in the total disturbance level), the time required to carry out measurements, the number and complexity of equipment needed, etc.
This chapter deal with the first of the two problems specified above - location of the disturbance source based on measurements made at a single point of a network (PCC), and does not concern an assessment of individual emission. Selected methods are presented for high harmonics, voltage fluctuations, voltage dips and unbalance, that allow determining location of the disturbance source: at the supplier side (upstream) or at the customer side (downstream), as viewed from PCC.

## 2. Voltage harmonics

The most commonly practical method for locating harmonic sources is based on determining the direction of active power flow for given harmonics, though many authors indicate its limitations e.g. [7,34,42,43]. Many other techniques are based on investigation of the "critical impedance" [21], the so-called voltage index value [32-34,41], interharmonic injection [42], determining voltage and current relative values [38], etc. Some methods determine the dominant harmonics source together with their quantitative contribution.
In most cases these methods, aside from their technical complexity, require precise information on values of equivalent parameters of the analysed system, which are difficultly accessible, or can only be obtained in result of costly measurements. As the examples some selected methods are more detail described below. They are presented employing the equivalent Thevenin circuit for the considered harmonic analysis (Fig. 2).

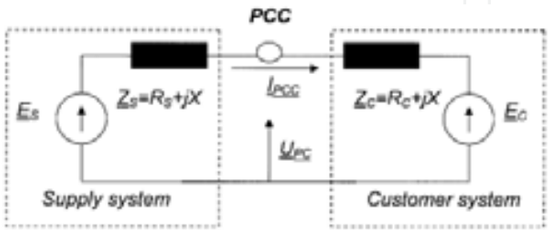


Fig. 2. Equivalent circuit for disturbance analysis $\underline{U}_{PCC}$, $\underline{I}_{PCC}$ - voltage and current values measured at PCC; $\underline{Z}_S$ , $\underline{Z}_C$ – equivalent impedances of the supplier and customer sides; $\underline{E}_S$ , $\underline{E}_C$ – harmonic voltages at the supplier and customer sides

### 2.1 The criterion of active power flow direction

The dominant source of the considered harmonic (h-th order) can be located analysing this harmonic active power ($P_h$) flow at PCC. Analysing the sign of this power at the measurement point we can conclude that:

- the positive sign of active power at PCC ($P_h>0$) means the dominant source of the considered harmonic is the supplier,
- the negative sign of active power at PCC ($P_h<0$) means the dominant source of the considered harmonic is the consumer.

A non-zero value of active power is the result of mutual interaction of the same frequency voltage and current, and is determined by the formula:

$$P_h = U_h I_h \cos\left(\Phi_{U_h} - \Phi_{I_h}\right) = U_h I_h \cos\varphi_h \tag{1}$$

where: $U_h$ and $I_h$ – rms voltage and current values of the h-th harmonic
$\Phi_{U_h}$ and $\Phi_{I_h}$ - the h-th harmonic current and voltage phase angles.

The method is equivalent to examining of the phase shift angle $\varphi_h$ between the considered harmonic voltage and current. If this angle is contained within the interval $-\pi/2 < \varphi < \pi/2$ then, according to this criterion, the dominant disturbance source is located at the supplier side. If the condition $\pi/2 < \varphi < 3\pi/2$ is fulfilled, the customer is the dominant source of the considered harmonic. For $\varphi = \pm\pi/2$ there is no decision about the dominant source of harmonic.

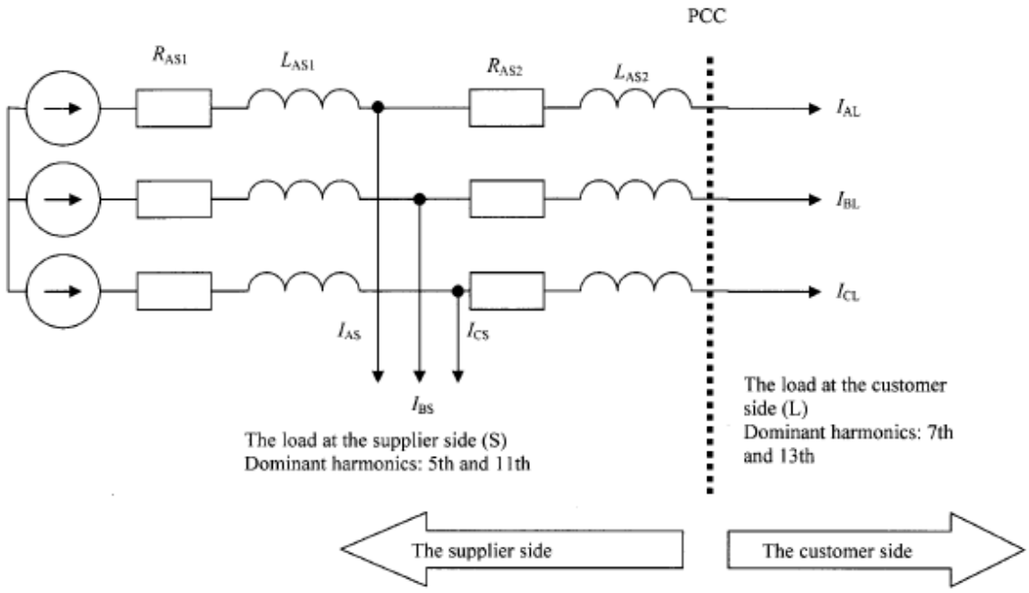


Fig. 3. Model of the electric power network chosen for simulations illustrating the active power flow method

Fig. 3 shows a simplified model of electric power network employed in the investigation, the supplier and customer sides are indicated. For the purpose of illustration let us assume the supplier is the dominant source of 5th and 11th harmonics and the customer is the dominant source of 7th and 13th harmonics. The above assumption is valid for both the

balanced and unbalanced system (Table 1). Balanced *RL* loads are connected in parallel with non-linear loads represented by currents $I_{iS}$, $I_{iL}$ for $i$ = A, B, C.

Fig. 4 summarizes the simulation results for selected cases. It is evident that in the case of balance for the considered harmonic the method correctly locates the dominant source of disturbance: at the supplier or customer side, also in the case where non-linear loads are connected at both sides of PCC

In the latter case a change in the phase shift angle between the current harmonics generated at the supplier and customer side may, in a certain interval of values, affect correctness of the inference about the disturbance source location. Fig. 6 shows the fifth harmonic active power variation at PCC for the case when the customer and supplier fifth harmonic relations were (a) 1:1.2 and (b) 1:1.8, and the phase shift angle between the 5th harmonic currents was varying within the interval 0-360$^0$. The larger the difference between the values of customer and supplier harmonic currents, the wider is the angle interval in which the inference is correct.

| $h$ | Phase A | | | | Phase B | | | | Phase C | | | |
|---|---|---|---|---|---|---|---|---|---|---|---|---|
| | Supplier | | Customer | | Supplier | | Customer | | Supplier | | Customer | |
| | $I_{\mathrm{m}}$[A] | $\varphi_{Ih}$[$^o$] | $I_{\mathrm{m}}$[A] | $\varphi_{Ih}$[$^o$] | $I_{\mathrm{m}}$[A] | $\varphi_{Ih}$[$^o$] | $I_{\mathrm{m}}$[A] | $\varphi_{Ih}$[$^o$] | $I_{\mathrm{m}}$[A] | $\varphi_{Ih}$[$^o$] | $I_{\mathrm{m}}$[A] | $\varphi_{Ih}$[$^o$] |
| 5 | 2.75/2.7 | 41/41 | 1.5/1.5 | 26/26 | 2.75/2.5 | 161/74 | 1.5/1.3 | 146/33 | 2.75/5 | 281/-123 | 1.5/2.7 | 266/-150.7 |
| 7 | 1/1 | -25/-25 | 2.3/2.3 | -15/-15 | 1/1.2 | -145/-15 | 2.3/1.6 | -135/-22 | 1/2.2 | -265/-160 | 2.3/3.9 | -255/167 |
| 11 | 1.6/1.6 | 100/100 | 0.9/0.9 | 79/79 | 1.6/1.35 | 220/199 | 0.9/1.1 | 199/96 | 1.6/1.9 | 340/-36 | 0.9/2 | 319/-91.6 |
| 13 | 0.2/0.2 | -75/-75 | 0.65/0.65 | -56/56 | 0.2/0.3 | -195/30 | 0.65/0.7 | -176/-77 | 0.2/0.3 | -315/172 | 0.6/1.4 | -296/112.7 |

Table 1. The supplier and customer harmonics – balanced/unbalanced system

Fig. 5 shows analogical simulations but for an unbalanced system. In the case of harmonic source located only at one side of PCC the calculated powers of harmonics in particular phases have different values but in the analysed case maintain the same sign and correctly indicate the source of disturbance.

In the case harmonic sources are located at both the supplier and customer side, the inference based on this method can not be correct. Comparison of simulation results in Fig. 5 with data contained in Table 1 indicates that the party responsible for 13th harmonic distortion was wrongly identified. The dominant party, responsible for the 13th harmonic presence in all phases is the customer, whereas the result of identification indicates the supplier in phases B and C. Thus the method fails also in the case of the considered circuit unbalance.

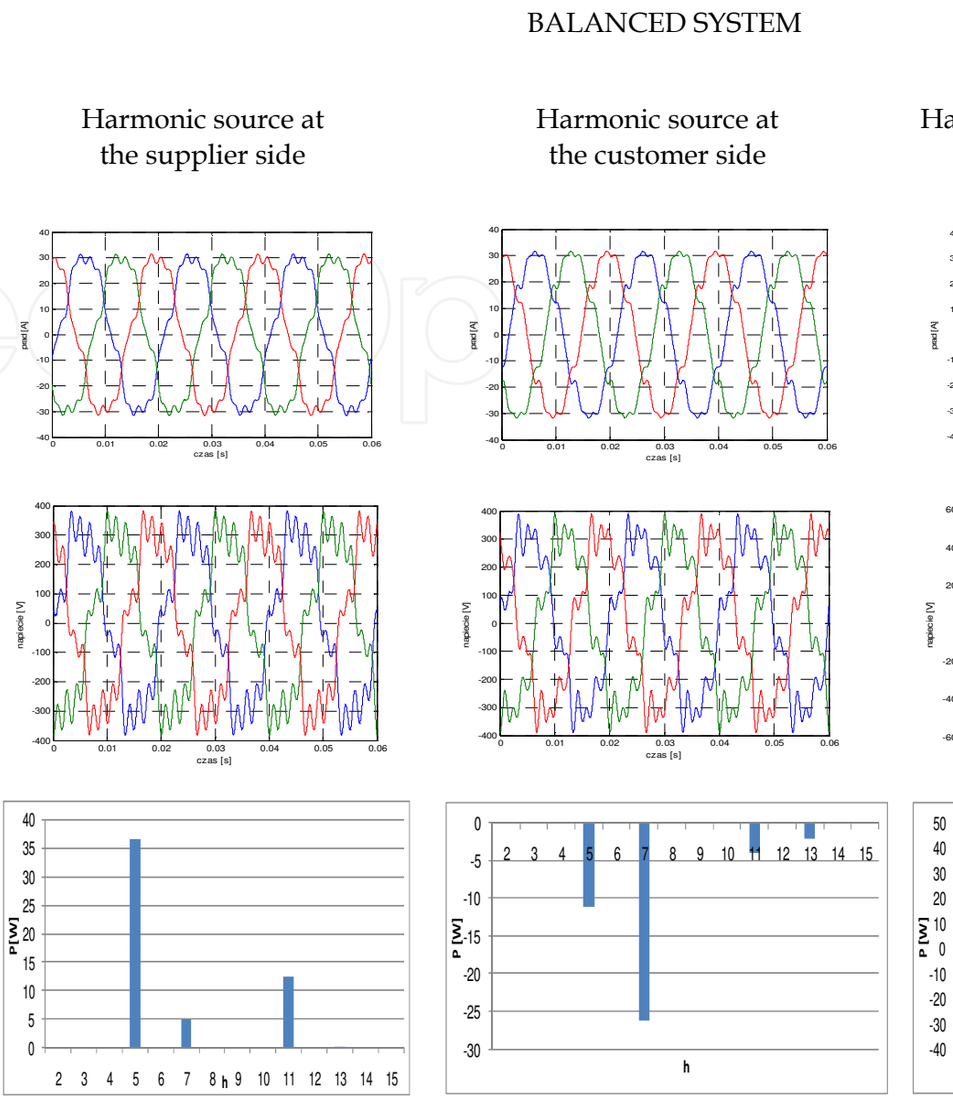


Fig. 4. The active power direction criterion for particular harmonics – example simulation results for a balanced system (Fig. 3)

UNBALANCED SYSTEM

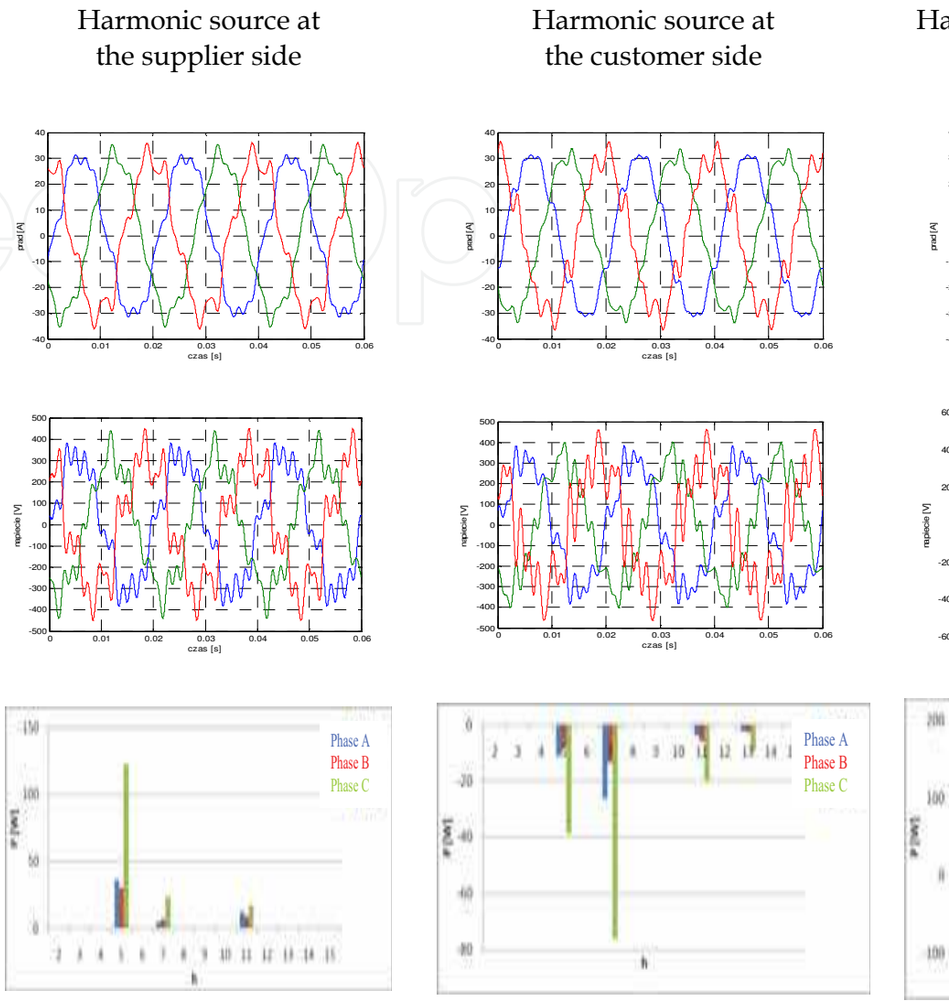


Fig. 5. The active power direction criterion for particular harmonics – example simulation results for an unbalanced system (Fig. 3)

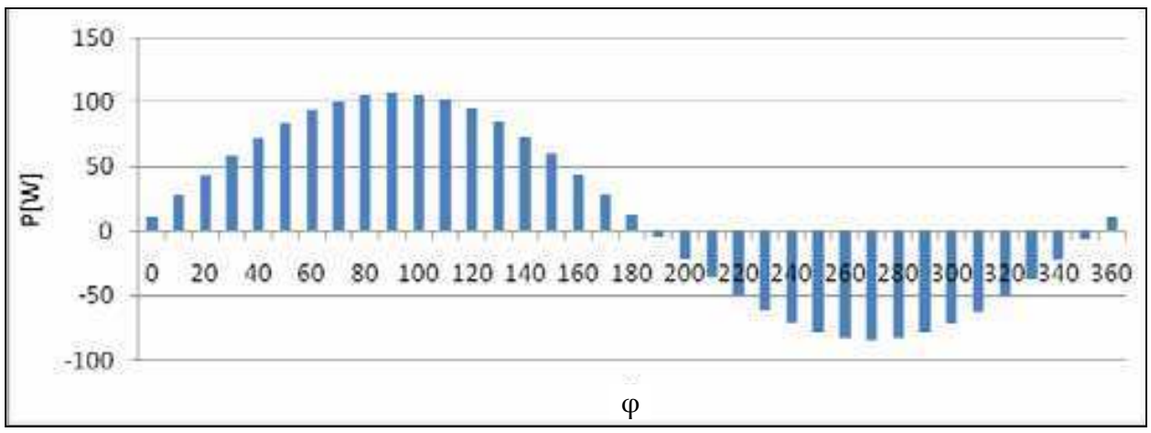


a)

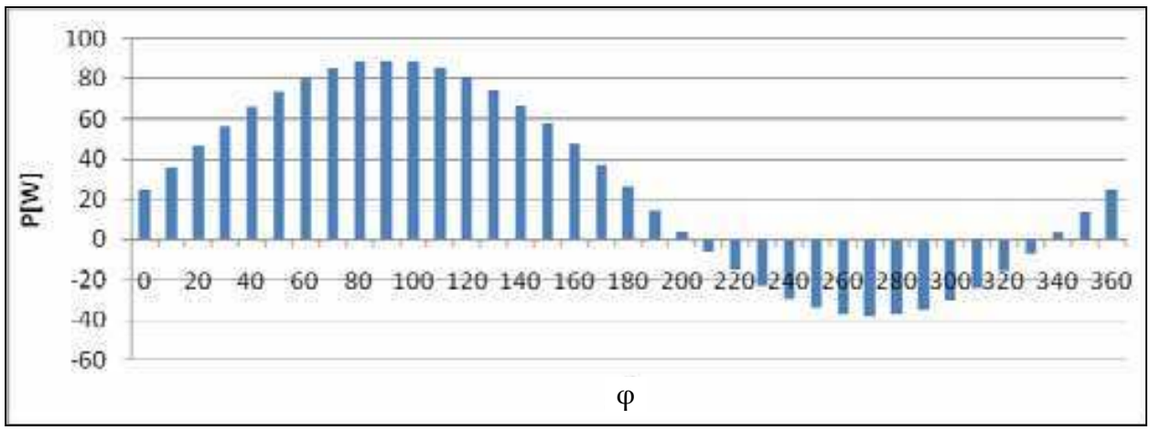


b)

Fig. 6. Variation of the 5th harmonic active power at PCC for different values of the phase shift angle φ between the customer and supplier current and various relations between their rms values: (a) 1:1.2; (b) 1:1.8

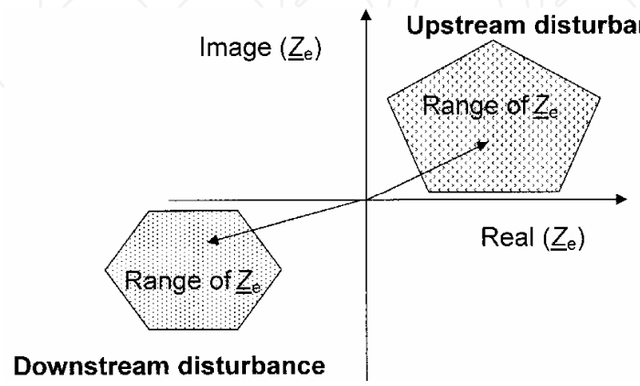


Fig. 7. Impedance plane illustration for result interpretation (criterion of the real part of the equivalent impedance at PCC – Chapter 2.2)

### 2.2 Criterion of the real part of the equivalent impedance at PCC [37]

The balance system of Fig. 1 can be represented by an equivalent one-phase circuit shown in Fig. 2. This is a *h*. harmonic circuit, $\underline{Z}_S$ and $\underline{E}_S$ are equivalent impedance and internal voltage source of the left side (supply system, upstream). $\underline{Z}_C$ and $\underline{E}_C$ are the similar parameters for the customer system on the right side.

Assume a disturbance occurs on the customer-side and leads to a voltage change at PCC (for considered harmonic), the measurements satisfy this equation before the occurrence of the event:

$$\underline{U}_{PCC} = \underline{E}_S - \underline{I}_{PCC}\underline{Z}_S \tag{2}$$

When a disturbance occurs, the voltage and current are changed to $\underline{U}_{PCC} + \Delta\underline{U}_{PCC}$ and $\underline{I}_{PCC} + \Delta\underline{I}_{PCC}$, where $\Delta\underline{U}_{PCC}$ and $\Delta\underline{I}_{PCC}$ are the voltage and current changes due to the customer-side event. If we assume that the parameters on the supply-side ($\underline{Z}_S$ and $\underline{E}_S$) remain unchanged during the disturbance period, a similar equation can be written as:

$$\underline{U}_{PCC} + \Delta\underline{U}_{PCC} = \underline{E}_S - \left(\underline{I}_{PCC} + \Delta\underline{I}_{PCC}\right)\underline{Z}_S \tag{3}$$

Since the probability that a disturbance occur on both sides simultaneously is practically zero, the above assumption that the parameters on the no disturbance side are constant is justifiable. Subtracting (2) from (3), we can find: the impedance of the no disturbance (supply) side as:

| | |
|---|---|
| the impedance of the no disturbance (supply) side | $\underline{Z}_S = -\dfrac{\Delta\underline{U}_{PCC}}{\Delta\underline{I}_{PCC}}$ |
| the customer-side impedance if a disturbance occurs on the supply-side | $\underline{Z}_C = \dfrac{\Delta\underline{U}_{PCC}}{\Delta\underline{I}_{PCC}}$ |

It can be seen that the quantity $\underline{Z}_e = \Delta\underline{U}_{PCC} / \Delta\underline{I}_{PCC}$ gives different signs depending on the origin of the disturbance. The basic idea is, therefore, to estimate $\underline{Z}_e$. In fact, $\underline{Z}_e$ has a physical meaning. It is the equivalent impedance of the no disturbance side. If the disturbance occurs on the supply-side, $\underline{Z}_e$ is the customer impedance. If the disturbance occurs on the customer-side, $\underline{Z}_e$ is the supply impedance multiplied by (-1). Since the resistance should always be positive, it is possible to determine the direction of harmonic source by checking the sign of the real part of the impedance $\underline{Z}_e$. This forms the basis of the method: calculate the equivalent impedance once a voltage disturbance is detected at monitoring point:

$$\underline{Z}_e = \frac{\Delta\underline{U}_{PCC}}{\Delta\underline{I}_{PCC}} = \frac{\underline{U}_{before} - \underline{U}_{after}}{\underline{I}_{before} - \underline{I}_{after}} \tag{4}$$

where ($\underline{U}_{before}$, $\underline{I}_{before}$) and ($\underline{U}_{after}$, $\underline{I}_{after}$) are pairs of pre-variation and after variation *h*. voltage and current harmonic, respectively. This gives rise to conclusions:

| | |
|---|---|
| If $Real\left(\underline{Z}_e\right) > 0$ | the source of *h*. harmonic is on supply-side |
| If $Real\left(\underline{Z}_e\right) < 0$ | the source of *h*. harmonic is on customer-side |

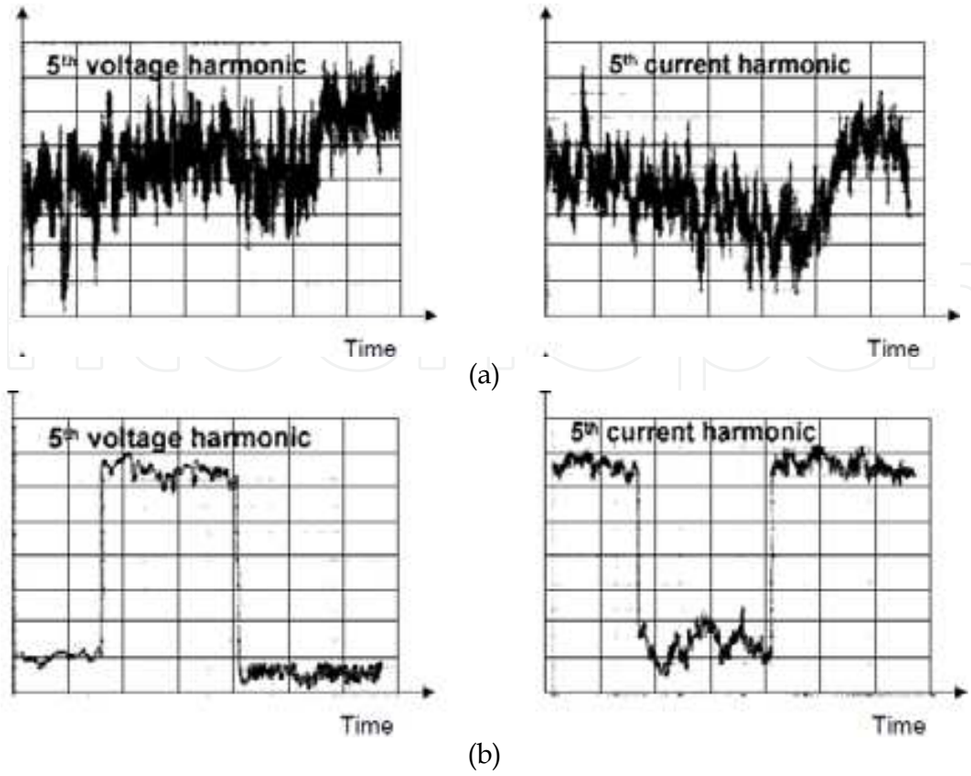


Fig. 8. (a) Unfavourable case: the 5 harmonic voltage and its variation are too small; (b) favourable case: the 5 harmonic variation is very significant [39]

The above method can be graphically illustrated on the impedance plane as shown in Fig. 7. If the calculated impedance $\underline{Z}_e$ lies in either the first or fourth quadrant ($R_e$ >0), the harmonic source is on the supply-side. And if the impedance lies in either the second or third quadrant ($R_e$ <0), the harmonic source is on the customer-side.
Because this method is based on harmonic variation, if the harmonic variation is too weak, it is very difficult to determine harmonic impedance with enough accuracy (Fig. 8).
The method drawbacks are: (a) high requirements for voltage and current harmonics measurement, especially with respect to their arguments; (b) time interval between measurements should be short (of the order of 1 - 3s) thus a large number of calculations is required; (c) accuracy of calculations can be solely achieved where the dominant harmonic source is at one side (either the supplier or the customer).

### 2.3 The "source" criterion [8,34]

The basis for the analysis is the equivalent circuit shown in Fig. 2, whose implication is the relation:

$$\underline{I}_{PCC} = \frac{\underline{E}_S - \underline{E}_C}{\underline{Z}_S + \underline{Z}_C} \quad \text{where: } \underline{E}_C = E_C \exp(j\varphi_C) \quad \underline{E}_S = E_S \exp(j\varphi_S) \tag{5}$$

The current at PCC can be represented by two components (Fig. 9):

$$\underline{I}_{PCC} = \underline{I}_{C-PCC} - \underline{I}_{S-PCC} \tag{6}$$

where $\underline{I}_{C-PCC}, \underline{I}_{S-PCC}$ are components associated with the customer and supplier side, respectively. The component $\underline{I}_{C-PCC}$ results from the *h*-th order harmonic source presence at the customer side, whereas the component $\underline{I}_{S-PCC}$ results from the *h*-th order harmonic source presence at the supplier side. The influence of a source located at the customer side on the current $\underline{I}_{PCC}$ is characterized by the projection of the current $\underline{I}_{C-PCC}$ vector onto the current $\underline{I}_{PCC}$ vector, whereas the influence of a source located at the supplier side – by the projection of the current $\underline{I}_{S-PCC}$ vector (Fig. 9).

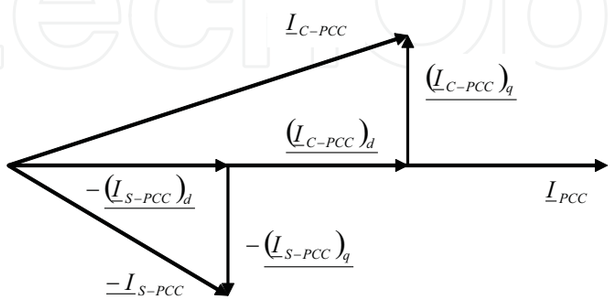


Fig. 9. Components of the current $\underline{I}_{PCC}$ at PCC [34]

As follows from Fig. 9:

$$\underline{I}_{C-PCC} = \sqrt{(I_{C-PCC})_d^2 + (I_{C-PCC})_q^2} \quad \underline{I}_{S-PCC} = \sqrt{(I_{S-PCC})_d^2 + (I_{S-PCC})_q^2} \tag{7}$$

and

$$(I_{C-PCC})_q = (I_{S-PCC})_q \tag{8}$$

The quotient of component modules $\underline{I}_{C-PCC}, \underline{I}_{S-PCC}$ is given by the formula:

$$\frac{I_{C-PCC}}{I_{S-PCC}} = \frac{\sqrt{(I_{C-PCC})_d^2 + (I_{C-PCC})_q^2}}{\sqrt{(I_{S-PCC})_d^2 + (I_{S-PCC})_q^2}} \tag{9}$$

Taking into consideration the relation 8 it can be concluded that the relationship between the component modules $\underline{I}_{C-PCC}$ and $\underline{I}_{S-PCC}$ is the same as the relationship between their projections onto the current $\underline{I}_{PCC}$ vector. It can be, therefore, concluded that if the projection of the current $\underline{I}_{C-PCC}$ vector onto the current $\underline{I}_{PCC}$ vector is greater than the projection of the current $\underline{I}_{S-PCC}$, i.e. the harmonic source at the customer side has a stronger influence on current $\underline{I}_{PCC}$ than the source at the supplier side, the condition:

$$\underline{I}_{C-PCC} \rangle \underline{I}_{S-PCC} \tag{10}$$

is fulfilled. Conversely: components $\underline{I}_{C-PCC}, \underline{I}_{S-PCC}$ can be determined using the relation:

$$\underline{I}_{C-PCC} = -\frac{\underline{E}_C}{\underline{Z}_S + \underline{Z}_C} \quad \underline{I}_{S-PCC} = \frac{\underline{E}_S}{\underline{Z}_S + \underline{Z}_C} \tag{11}$$

Thus the following relations are true:

| | | |
|---|---|---|
| If $\underline{I}_{C-PCC} \rangle \underline{I}_{S-PCC}$ then $E_C \rangle E_S$ | the dominant disturbance source is located at the customer side | |
| If $E_C = E_S$ | there is no decision about the dominant source of harmonic | (12) |
| If $\underline{I}_{C-PCC} \langle \underline{I}_{S-PCC}$ then $E_C \langle E_S$ | the dominant disturbance source is located at the supplier side | |

According to the considered criterion the inference is based on source voltages $\underline{E}_C$ and $\underline{E}_S$, that are unknown. They can be determined from voltages and currents measured at PCC and the knowledge of equivalent impedances $\underline{Z}_C$ and $\underline{Z}_S$:

$$\underline{U}_{PCC} = \underline{E}_S - \underline{I}_{PCC}\underline{Z}_S = \underline{E}_C + \underline{I}_{PCC}\underline{Z}_C \tag{13}$$

However, the internal impedances of equivalent harmonic sources, representing the supplier and customer sides, are also unknown and their determination is not an easy task, it is significant disadvantage of this method.

### 2.4 The "critical impedance" criterion

The authors of publication [21] observed in a power system shown in Fig. 2 a strong association between the sign of reactive power and the relation between source voltages modules $\underline{E}_S$ and $\underline{E}_C$. This is explained by the formula determining the source $E_S$ active and reactive power values in the case where the circuit equivalent resistance is negligibly small:

$$P = E_S I_{PCC} \cos\Theta = \frac{E_S E_C}{X} \sin\delta \tag{14}$$

$$Q = E_S I_{PCC} \sin\Theta = \frac{E_S}{X}\left(E_C \cos\delta - E_S\right) \tag{15}$$

where: $R = \mathrm{Re}(\underline{Z})$, $X = \mathrm{Im}(\underline{Z})$, $\underline{Z} = \underline{Z}_S + \underline{Z}_C$, $\underline{Z}_C = R_C + jX_C$, $\underline{Z}_S = R_S + jX_S$

$\Theta = \arg\underline{E}_S - \arg\underline{I}_{PCC}$, $\delta = \arg\underline{E}_C - \arg\underline{E}_S$

According to (14), the direction of active power flow (i.e. its sign) is exclusively determined by phase angles of voltages at both: the supply and load end of a line, and does not depend on the relation between modules of voltages $E_C$ and $E_S$. This relation, however, determines the sign of reactive power. It is noticeable from relations (15) that if $Q$>0, then $E_C$ > $E_S$, i.e. the dominant source of the considered current harmonic at PCC is a source at the customer side. Because of the presence of $\cos\delta$ in the formula (15) it cannot be concluded that if $Q$<0 then $E_C$ < $E_S$, i.e. the supplier is the dominant source of the considered current harmonic. Publication [21] gives theoretical basis for the decision making process utilizing the examination of reactive power also if $Q$<0 introducing the concept of the so-called critical impedance.

The base of this method is finding the answer to the question: how far the reactive power generated by the source $E_S$ can "flow" along the impedance $jX$, assuming this impedance is distributed evenly between the sources $E_S$ and $E_C$. In order to find the answer has been defined the voltage value at an arbitrary point $m$ between sources $E_S$ and $E_C$ (Fig. 2):

$$\underline{U}_m = \frac{X_1}{X_1 + X_2}\underline{E}_S + \frac{X_2}{X_1 + X_2}\underline{E}_C \tag{16}$$

where: $X = X_1 + X_2$, and $X_2$ is the part of $X$ at the source $E_S$ side. The point of the least voltage $U_m$ value can be determined from the condition $\frac{\partial U_m}{\partial X_2} = 0$:

$$x = \frac{E_S^2 - E_S E_C \cos\delta}{E_S^2 + E_C^2 - 2E_S E_C \cos\delta} X \tag{17}$$

where $x$ is the reactance of the source $E_S$ for the point of the least voltage value. It is noticeable that:

$$I_{PCC}^2 = \frac{E_S^2 + E_C^2 - 2E_S E_C \cos\delta}{X} \tag{18}$$

Regarding (15) and (18), we have:

$$x = \frac{-Q}{I_{PCC}^2} = -\frac{E_S}{I_{PCC}} \sin\Theta \tag{19}$$

As inferred from the formula (19) $x$ is the most distant point to which the reactive power generated by the source $E_S$ can "flow". If the point $x$ is closer to the customer side ($x > X/2$) then the dominant source of the considered harmonic is located at the supplier side. If $x < X/2$ then $E_C$ is the dominant source.
The so-called critical impedance *CI*, which is the basis for inferring in this method, is defined in [21]:

$$CI = 2\frac{Q}{I_{PCC}^2} \tag{20}$$

Taking into account the circuit equivalent resistance ($R \neq 0$), [21] gave this concept a practical value. Thus the relations (14) and (15) take the form:

$$P = \frac{E_S E_C}{X}\sin(\delta + \beta) - \frac{E_S^2}{Z}\sin\beta \qquad Q = \frac{E_S E_C}{X}\left(\cos(\delta + \beta) = \frac{E_S^2}{Z}\cos\beta\right) \tag{21}$$

where: $\beta = arctg\frac{R}{X}$. Using transformation of powers expressed by (22) [34]:

$$\begin{bmatrix} P^* \\ Q^* \end{bmatrix} = T\begin{bmatrix} P \\ Q \end{bmatrix} = \begin{bmatrix} \frac{E_S E_C}{Z}\sin\delta \\ \frac{E_S E_C}{Z}\cos\delta - \frac{E_S^2}{Z} \end{bmatrix} \text{ where } \begin{bmatrix} \cos\beta & -\sin\beta \\ \sin\beta & \cos\beta \end{bmatrix} \tag{22}$$

we obtain the same relations that describe the active and reactive power as for the condition $R$=0 and the basis for inference about location of the dominant harmonic source remains true. Then the index *CI* is given by relation:

$$CI^{*} = 2\frac{E_S}{I_{PCC}}\sin(\Theta+\beta) \tag{23}$$

This index is determined from the voltage and current measurements at PCC, which are utilized for the source voltage $\underline{E}_S$ calculation:

$$\underline{E}_S = \underline{U} + \underline{I}_{PCC}\underline{Z}_S \tag{24}$$

The impedance $\underline{Z}_S$, which occurs in (24) is not always exactly known. In consequence, the source voltage $\underline{E}_S$ may not be determined accurately. Another quantity that occurs in the formula for *CI* (23), which is inaccurately determined when the impedance $\underline{Z}_S$ and, above all, the impedance $\underline{Z}_C$ are not exactly known, is the angle $\beta$. The above factors cause that decisions taken according to the criterion (25) may not be correct.

| | | |
|---|---|---|
| If | $CI > 0$ or $CI < 0$ and $\lvert CI\rvert < Z_{\min}$ | the dominant source of the considered harmonic is located at the customer side |
| If | $Z_{\min} < \lvert CI\rvert < Z_{\max}$ | there is no decision about the dominant source of the considered harmonic |
| If | $CI < 0$ and $\lvert CI\rvert > Z_{\max}$ | the dominant source of the considered harmonic is located at the supplier side |

(25)

where $Z_{\min}, Z_{\max}$ determine the interval of impedance *Z* changes.

### 2.5 The voltage indicator criterion [34]

The method is based on the equivalent circuit diagram presented in Fig. 2, created for the investigated harmonic. By investigating the quotient of source voltages of the supplier's and the consumer's side, known as "voltage indicator"[1]:

$$\Theta_U = \frac{E_C}{E_S} = \frac{\lvert\underline{Z}+\underline{Z}_C\rvert}{\lvert\underline{Z}-\underline{Z}_S\rvert} \quad \text{where } \underline{Z} = \frac{\underline{U}_{PCC}}{\underline{I}_{PCC}} \tag{26}$$

it is possible to determine the location of the dominant distortion source in the electrical power network, according to the following criterion:

| | | |
|---|---|---|
| If | $\Theta_U > 1$ | the dominant source of the investigated harmonics is located at the consumer's side |
| If | $\Theta_U = 1$ | it is impossible to explicitly identify the location of the dominant source of the disturbance |
| If | $\Theta_U < 1$ | the dominant source of the investigated harmonics is located at the supplier's side |

(27)

Impedance values $\underline{Z}_S$ and $\underline{Z}_C$ have been assumed as known. Since this requirement is difficult to meet, the criterion is modified to the form (28), which takes into account approximate knowledge of equivalent impedance values $\underline{Z}_S$ and $\underline{Z}_C$. The ranges are determined which may contain the values of such impedances, evaluated on the basis of the

[1]A detailed theoretical justification of the method is to be found in works [32,33,34,41].

analysis of various operating conditions of an investigated electrical power system. Impedance $\underline{Z}_x$ variation range where $x \in (C,S)$ is defined by means of equations: $Z_{x\min} \le Z_{xn} \le Z_{x\max}$ and $\alpha_{x\min} \le \alpha_{xn} \le \alpha_{x\max}$, where $Z_{xn}, \alpha_{xn}$ are the modulus and the argument, respectively, of the impedance $\underline{Z}_x$. On this basis, indicator extreme values $\Theta_{U\min}$ and $\Theta_{U\max}$, are determined, which are the basis for the following conclusions:

| | | | |
|---|---|---|---|
| If | $\Theta_{U\min} \rangle 1$ | the dominant source of the investigated harmonics is located at the consumer's side | |
| If | $\Theta_{U\min} \langle 1 \langle \Theta_{U\max}$ | it is impossible to explicitly identify the location of the dominant source of the disturbance | (28) |
| If | $\Theta_{U\max} \langle 1$ | the dominant source of the investigated harmonic is located at the supplier's side | |

The results of example simulations illustrating this method (according with Fig. 3 and Table 1) are presented in Fig. 10. Fig. 11 shows the results of the identification of the disturbance source by means of the voltage indicator method, depending on the phase shift angle between 5 harmonic current of the supplier and the consumer for two distinct relations between rms values of these currents. The change of phase shift angle value does not affect the correctness of conclusions in the analysed case.

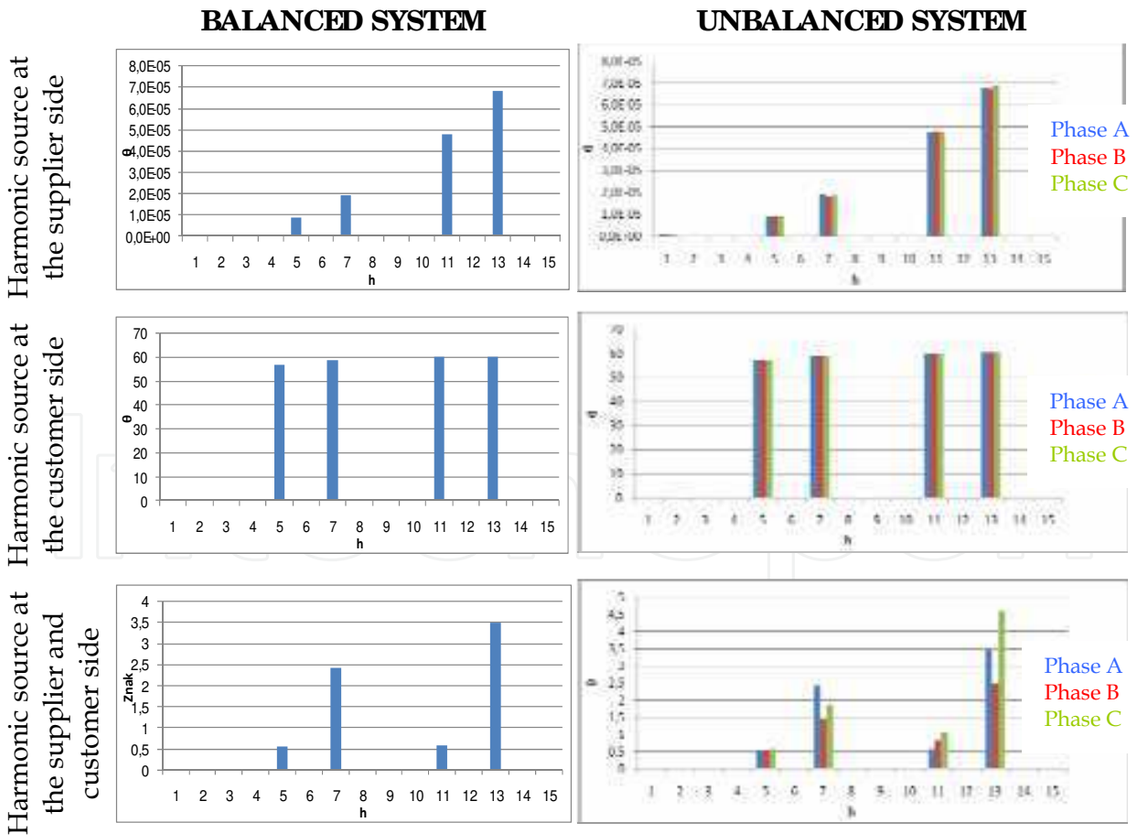


Fig. 10. Criterion of voltage indicator – example results of simulations for a system as that presented in Fig. 3

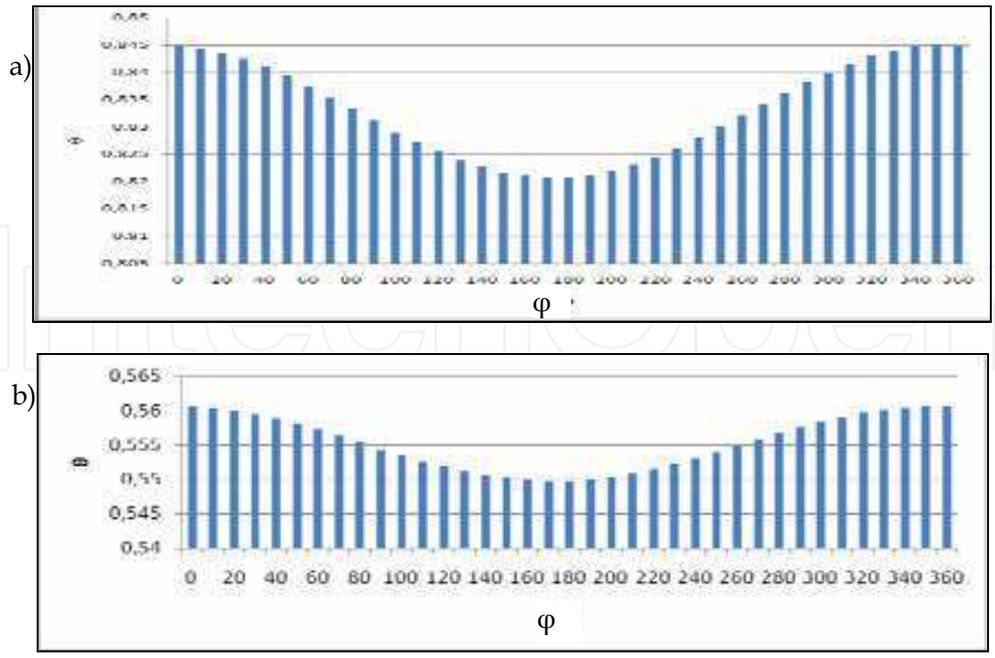


Fig. 11. Variation of 5th harmonic active power value for various values of phase shift angle φ between the supplier's and the consumer's current harmonic and for various relations between their rms values: (a) 1:1,2; (b) 1:1,8

### 2.6 Criterion of the relative values of voltage and current harmonics [38]

This method consists in comparison of relative harmonic values measured with respect to the fundamental voltage and current values. While analysing the correctness of decisions made on the basis of this method the equivalent circuit diagram of an electrical power system, presented in Fig. 2, is used In the case of a single harmonic source, located, for example, at the energy supplier's side, the following equations are valid:

for the fundamental component – index (1)

$$\underline{U}_{PCC(1)} = \underline{E}_{S(1)} - \underline{I}_{PCC(1)}\underline{Z}_{S(1)} = \underline{I}_{PCC(1)}\underline{Z}_{C(1)}$$

for *h*. harmonic

$$U_{PCCh} = \underline{E}_{Sh} - \underline{I}_{PCCh}\underline{Z}_{Sh} = \underline{I}_{PCCh}\underline{Z}_{Ch}$$

Therefore, voltage quotient:

$$\frac{U_{PCCh}}{U_{PCC(1)}} = \frac{I_{PCCh}Z_{Ch}}{I_{PCC(1)}Z_{C(1)}} = \frac{I_{PCCh}}{I_{PCC(1)}}\left|\frac{\underline{Z}_{Ch}}{\underline{Z}_{C(1)}}\right| = \frac{I_{PCCh}}{I_{PCC(1)}}K \tag{29}$$

Assuming that:

$$\underline{Z}_{C(1)} = R_{C(1)} + jX_{C(1)} \text{ and } \underline{Z}_{Ch} = R_{C(1)} + jhX_{C(1)} \tag{30}$$

for $h$ >1 the following inequality is satisfied: $\sqrt{R_{C(1)} + h^2X_{C(1)}^2} \rangle \sqrt{R_{C(1)} + X_{C(1)}^2}$ which means that $K$ >1 and, as a result $\frac{U_{PCCh}}{U_{PCC(1)}} \rangle \frac{I_{PCCh}}{I_{PCC(1)}}$. A similar reasoning may be carried out for the case when a single harmonic source is located at the consumer's side and for sources located at both sides of the PCC [34]. In each case the conclusion criterion is based on the relations (for $h$= 2,3,4 …):

$$\frac{U_{PCCh}}{U_{PCC(1)}} \geq \frac{I_{PCCh}}{I_{PCC(1)}}$$ The dominant harmonic source is located at the supplier's side

$$\frac{U_{PCCh}}{U_{PCC(1)}} < \frac{I_{PCCh}}{I_{PCC(1)}}$$ The dominant harmonic source is located at the consumer's side

The above reasoning is correct if equation (30) is approximately valid.

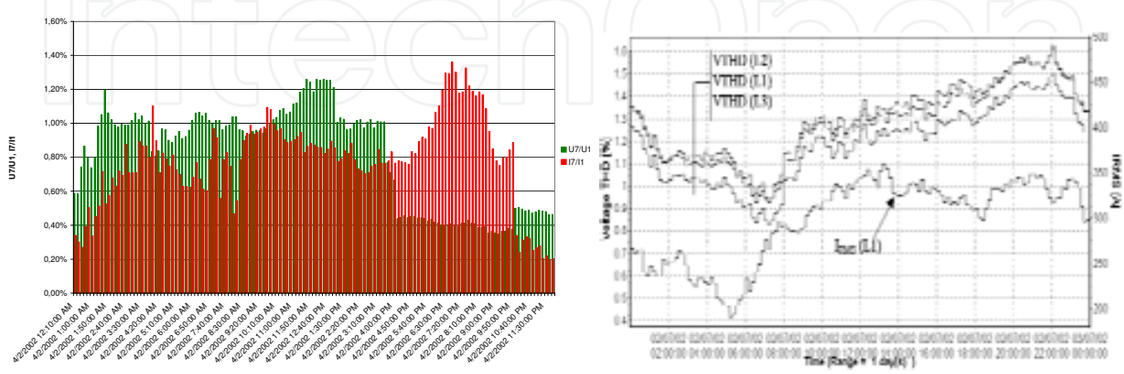


(a) (b)

Fig. 12. (a) Relative values of the 7th voltage and current harmonic in phase L3; (b) the change in the phase-to-neutral voltages distortion factor during an example workday 24 hours (110kV network)

It happens that the influence of some harmonics on the voltage to current ratio is increased due to the resonance, and therefore the above relations are amplified or reduced. For the above reasons it is essential that harmonics should be analysed comprehensively, taking into consideration several lowest, especially odd harmonics from the 3rd to 11th, on which the impedance from the supply side has the lowest influence. An example of the 7th harmonic measurements at the feed point of 110 kV distribution network in large city is shown in Fig. 12a. A dominant influence of the municipal network loads during evening hours is evident and confirmed by the daily THD time characteristic, measured at the same point (Fig. 12b).

### 2.7 Statistical approach from simultaneous measurement of voltage and current harmonics [13]

Voltage and current harmonics are measured simultaneously at the point of evaluation during longer periods of time - Fig. 13 (10-minutes values, measured during one week).

In Fig. 13a, the experimental points are spread over the area delimited by the two straight lines. This means that the harmonic current and the resulting voltage are actually resulting from the combined influences of the background level and the considered distorting load, without any prevalence of one or the other. In Fig. 13b, however the load acts clearly as a rather dominant emitter at the PCC: the points are mostly grouped along the straight line. This means that the influence of the considered installation is greater than the background harmonic level.

A similar reasoning may be based on the investigation of the correlation between voltage harmonic value and, for instance, current rms value or active power.

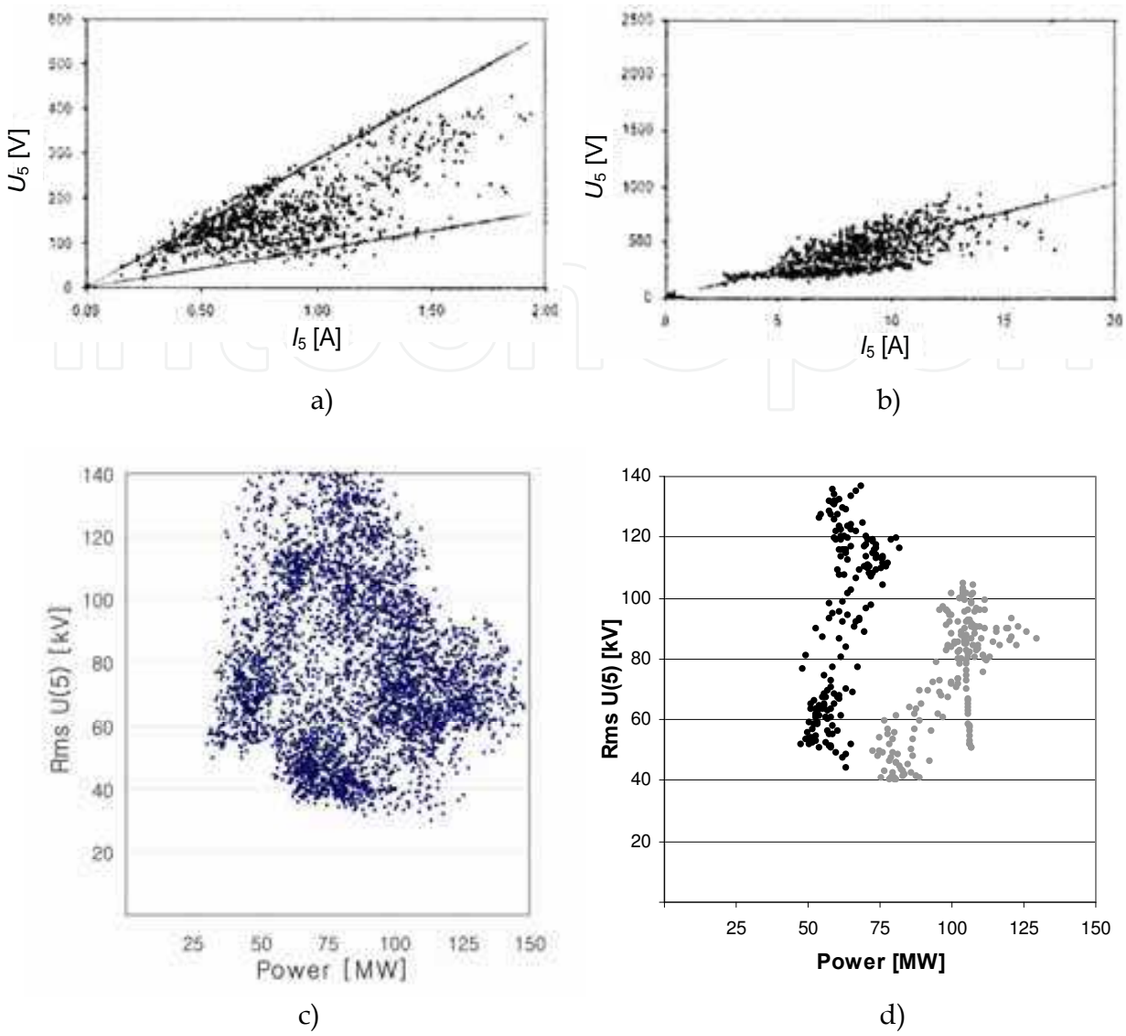


Fig. 13. Examples of: 5th voltage harmonic vs. (a,b) 5th current harmonic and (c,d) active power of a large industrial company fed from 110 kV line - 4 months of measurement (d), selected days of operation that shows a load acting as a dominant emitter (gray dots) and the supply that acts as a dominant emitter (black dots)

## 3. Voltage dips

The procedure of locating the dip source is usually a two-stage technique. The first part involves inferring whether the dip has occurred upstream or downstream of the measuring point, i.e. at the supplier's or the consumer's side. In the next step the algorithm that precisely computes the voltage dip location is applied. This chapter deals with the first stage. Even though a methodology for the exact locations of voltage dips does not exist yet, several methods for voltage dip source detection have already been reported. They are based mainly on: the analysis of voltage and current waveforms; the analysis of the system operation trajectory during the dip; the analysis of the equivalent electric circuit; the analysis of power and energy during the disturbance; the analysis of voltages; asymmetry factor value and symmetric component phase angle and algorithms for the operation of protection

automatics systems (impedance variation analysis, the analysis of current real part, "distance" protection).

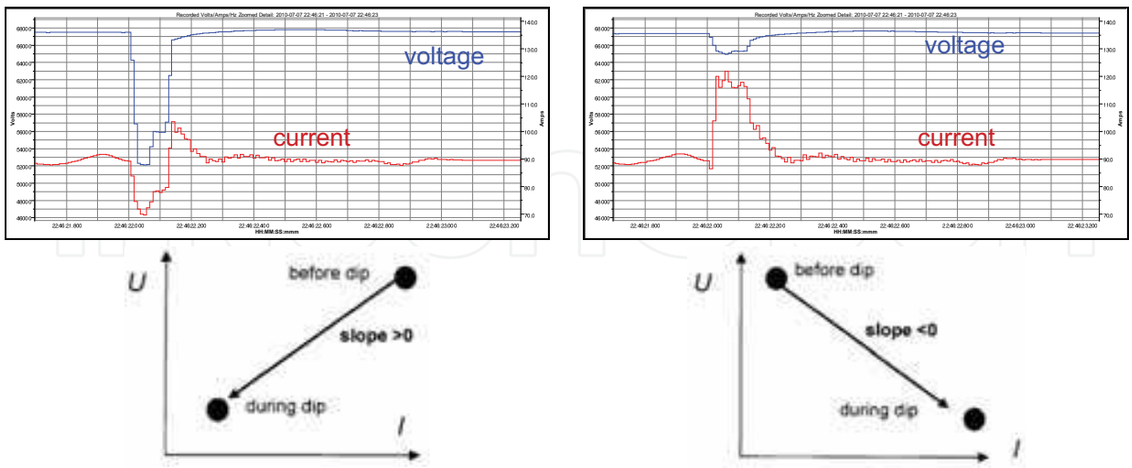


Fig. 14. Slope of the trajectory line of the (U-I) system during the dip for various short circuit locations: a) upstream (point A at Fig. 1), b) downstream (point B at Fig. 1)

### 3.1 Analysis of the voltage and current waveforms at PCC

The location of the point of connection of the motor whose start causes a disturbance (in general: a voltage dip source) can be sometimes identified with respect to the considered point of a supply network (the measurement point) on the basis of recorded voltages and currents — Fig. 14. A noticeable increase in the current during a voltage dip may indicate that the cause of a disturbance is located downstream the monitoring point (Fig. 14b). That does not always hold true. At reduced voltage the current of induction motor loaded with a constant torque increases, although, as a rule, it is smaller than the increase necessary to cause a voltage dip. Similarly, the increase of current can result from the voltage control at the consumer's side or the response a power electronic interface control.

### 3.2 The criterion using the system operating conditions trajectory during the dip

The natural consequence of waveform analysis during the disturbance is an empirical method based on the investigation of the trajectory of the supply system operation point before and during the disturbance [22].

In the example used to illustrate this method it has been assumed that there is one source supplying a passive load, while the monitoring device is connected in the PCC point (Fig.1). Two cases of three-phase short circuits have been investigated: in points A and B, which result in a voltage dip. Both short circuits lead to voltage reduction in point PCC; however, current value variation will be different in each case.

During the short circuit in point A the current measured in point PCC will be typically lower in comparison with its value before the disturbance occurred. In the other case (short circuit in point B) the current measured in point PCC will be the sum of short-circuit current and load current during the dip. Its value will be higher than before the disturbance occurrence.

The above statements are also illustrated in Fig. 14. Particular operating conditions of the supply system are presented by means of points representing voltage and current before and after the dip. The sign of derivative of the segment joining these two points makes it possible to identify the short circuit location: a positive derivative suggests the short circuit at the source side (in point A), while a negative derivative suggests the short circuit at the load side (in point B). Although originally the method was intended for a system with a single supply source, it can also be applied, after small modifications, to two-side supply systems, such as that presented in Fig. 15 (also including non-linear elements) [22].
In this case the disturbance source location is determined in relation to the assumed direction of active power flow in the measurement point. If the disturbance source is located on the right side of the measurement point (i.e. in the same direction as that of active power flow) it means it is located at the "lower" side. Disturbances on the left side of the measurement point (the direction is opposite to that of active power flow) indicate that the source is located at the "upper"side.

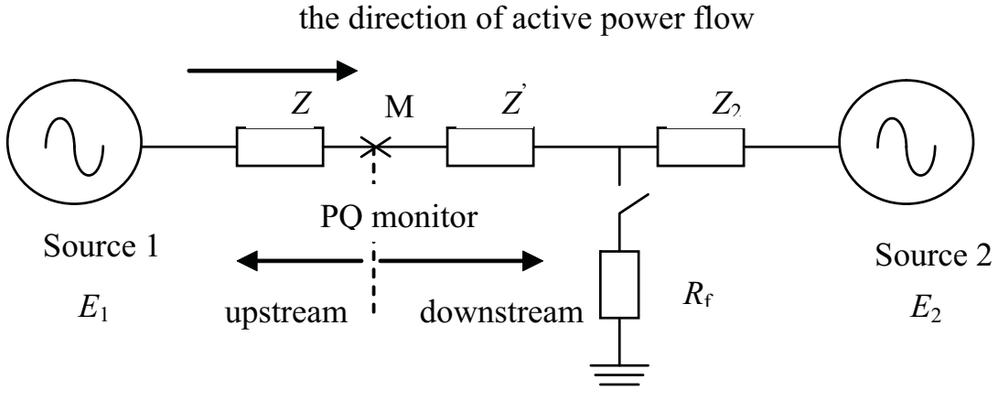


Fig. 15. A two-source system locating the dip source [22]

Fig. 15 shows a short circuit (represented by resistance $R_f$), which occurs on the right side of the measurement point, while those elements of the equivalent circuit diagram which are on the left side remain unchanged. Voltage in the measurement point (which is not PCC) can be expressed by the equation:

$$\underline{U} = \underline{E_1} - \underline{I}\underline{Z} \tag{31}$$

where $\underline{U}$ and $\underline{I}$ can be measured directly in point M. Multiplying both sides of equation (31) by current conjugate value $\underline{I}^*$, and taking into account only the real part, results in the following equation:

$$UI\cos\theta_2 = E_1 I\cos\theta_1 - I^2 R \tag{32}$$

where $\theta_2$ – phase angle between vectors $\underline{U}$ and $\underline{I}$, $\theta_1$ – phase angle between $\underline{E}_1$ i $\underline{I}$, $R$ represents the real part of complex impedance $\underline{Z}$. Transforming (32) to the form:

$$U\cos\theta_2 = -IR + E_1\cos\theta_1 \tag{33}$$

results in the equation, the form of which is convenient to determine the inclination of the *U-I* trajectory. For example, if $\cos\Theta_2 \rangle 0$, the direction of active power flow is such as has been assumed, i.e. such as has been shown in Fig. 15, while the disturbance source is located at the lower side and $|U\cos\Theta_2| = U\cos\Theta_2$. Each point representing the system operating conditions in coordinate system ($I$, $|U\cos\Theta_2|$) is placed on the straight line with the inclination $-R$, like in Fig. 16a (assuming that $\cos\theta_1$ does not significantly change its value).

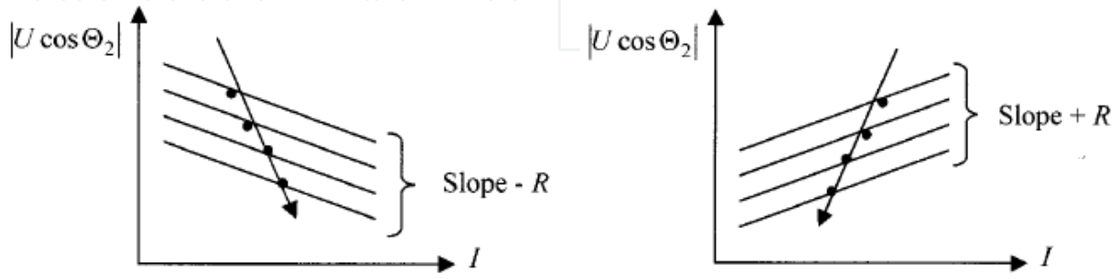


a) b)

Fig. 16. The slope of system trajectory during the disturbance: the disturbance source is located (a) downstream, (b) upstream the measurement point [22]

If $\cos\Theta_2 \langle 0$, active power flows from $E_2$ to $E_1$, the disturbance is located at the upper side, and the equation has the following form:

$$U\cos\theta_2 = IR - E_1\cos\theta_1 \tag{34}$$

Every point representing the system operating conditions in coordinate system ($I$, $|U\cos\Theta_2|$) is placed on the straight line with the slope $+R$ (Fig. 16b). The line which is connecting these points during the disturbance has positive inclination then – providing $\cos\theta_1$ does not significantly change its value during the disturbance.

It can be demonstrated that during the disturbance $|\cos\theta_1|$ usually decreases when current $I$ increases for the disturbance source at the lower side and decreases for the upper side. This ensures that in practical cases conclusions are drawn in the correct way.

It has been assumed so far that the direction of active power flow does not change before and after the disturbance occurrence, which is not always the case. Variations are possible, however, only in the case of disturbances at the upper side, while for disturbances at the lower side the direction of active power flow remains unchanged. This fact may be used for the identification of voltage dip source location: if the direction of active power flow changes, the event must have occurred at the upper side. This additional hint, together with the identification of the inclination of the trajectory *U-I* during the dip may help draw correct conclusions.

The investigated method has been used in simulation studies, the aim of which was to locate the voltage dip source using a modified model of *IEEE 37-Node Test Feeder* network [18]. Its diagram is presented in Fig. 17a. A three-phase short circuit, which occurred in node 703, has been simulated; the study investigated if the disturbance in nodes 702 and 709 was located correctly (Fig. 17b).

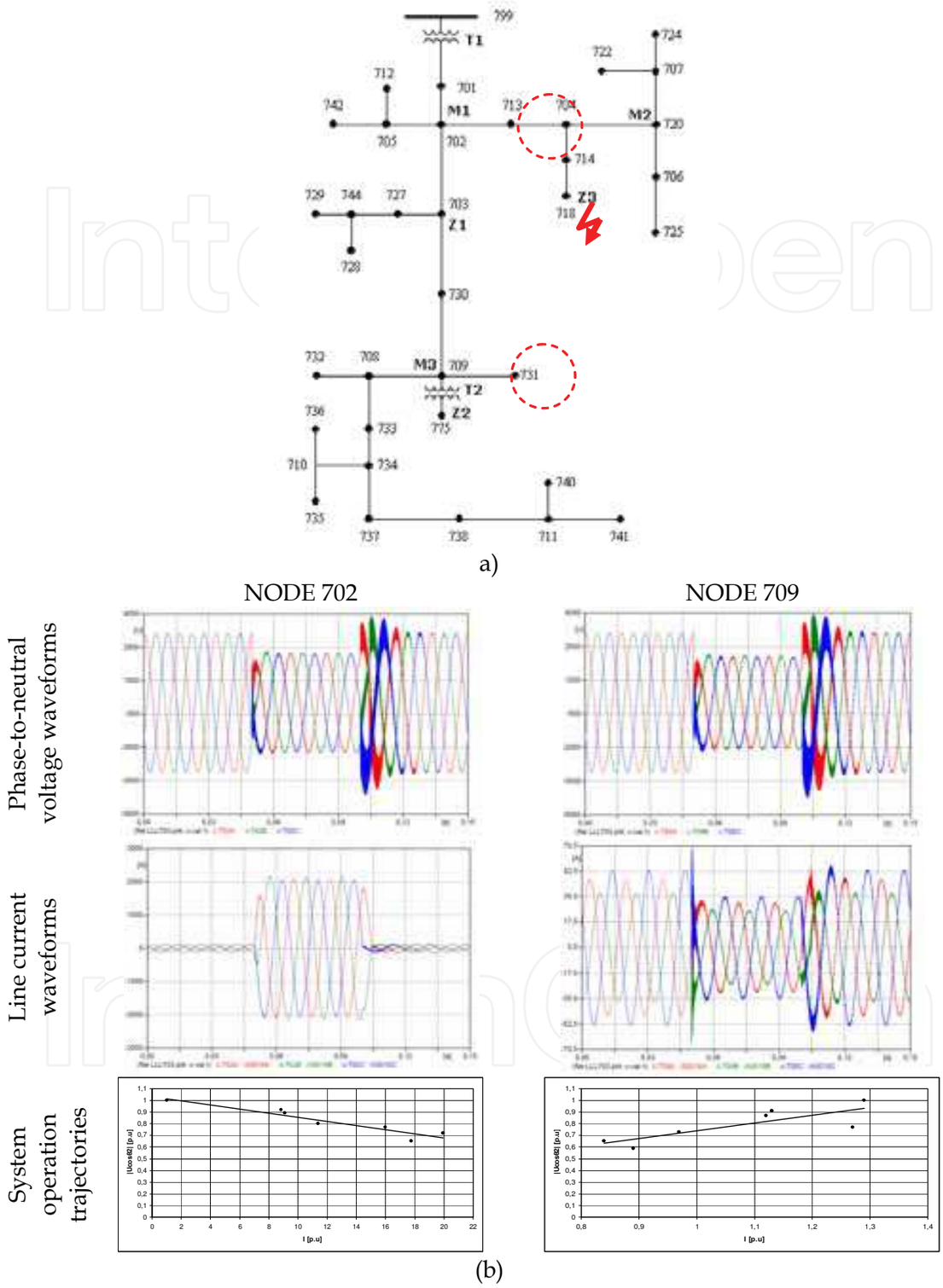


Fig. 17. Example results of a three-phase short circuit simulation in node 703 of 23 network model; waveforms of voltages and currents in nodes 702 and 709 as well as system operation trajectories in these points for phase L1 (analogous waveforms in other phases)

Both this and other simulation studies have confirmed that it is highly probable to draw correct conclusions concerning the dip source location in the case of symmetrical disturbances; incorrect conclusions can be drawn in the case of asymmetrical disturbances, in particular single-phase earth faults.

### 3.3 The analysis of the equivalent electric circuit

In the investigated point of the supply system, both current and voltages are measured at the same time. The measured current is the basis for calculating the voltage value on the basis of the equivalent circuit diagram of the studied system. Conclusions concerning the disturbance location are drawn on the basis of the relationship between the measured ($U_m$) and the calculated ($U_S$) voltage value in PCC (Fig. 18). If the relationship is $U_S \approx U_m$, it means that the disturbance source is located "downstream" the measurement point (at the consumer's side), whereas if $U_S << U_m$, the disturbance source is located at the supplier's side.

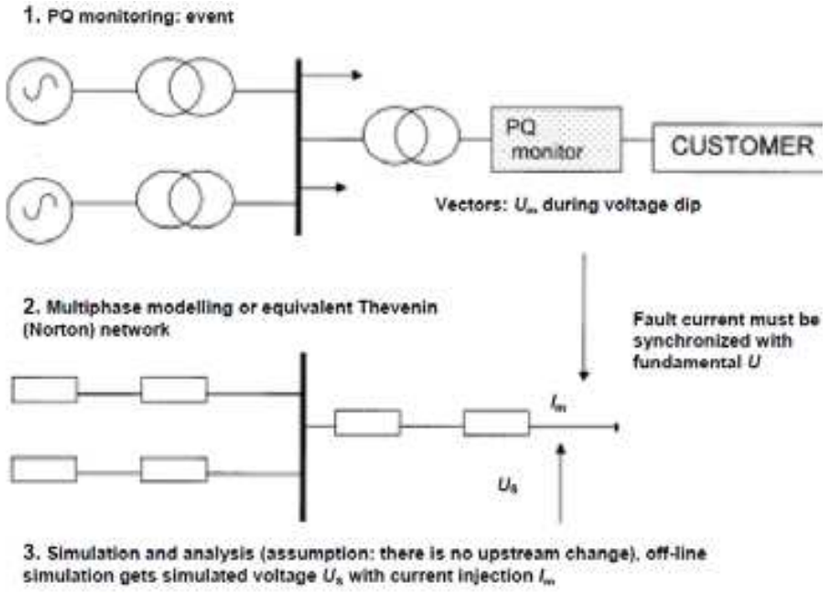


Fig. 18. The method of dip source location on the basis of the comparison between measured and calculated voltage variation value in PCC [39]

### 3.4 The criterion using power and energy during the disturbance

The circuit of a short-circuit which has occurred at the consumer's side takes power from the supply network. On the other hand, during a short circuit that has occurred at the supplier's side energy in transient state will flow from the consumer's side. The direction of flow of instantaneous power and energy is determined on the basis of registered voltage and current waveforms.

In the steady state, assuming that the network is a symmetrical one, instantaneous power has practically constant value which changes as a result of variations in voltage and current instantaneous waveforms. The difference in power between the steady state and the disturbance state is the so-called "disturbance power" - DP. According to this definition, in the steady state the DP value approximately equals zero (assuming very brief intervals between subsequent measurements), while during short circuit it is different than zero.

As a result of integrating the DP value, disturbance energy – DE – is determined. Information concerning DP and DE variation makes it possible to locate the voltage dip source, because during a short circuit energy flows towards the place of the short circuit occurrence (Fig. 19) – the increase of DE during the disturbance indicates that the disturbance source is located downstream the measurement point. On the other hand, DE decreases if the disturbance source is located upstream the measurement point [33]. The method requires that a threshold value of energy is assumed; since the reliability of results depends on this value, the method works correctly as long as the value has been accurately chosen.

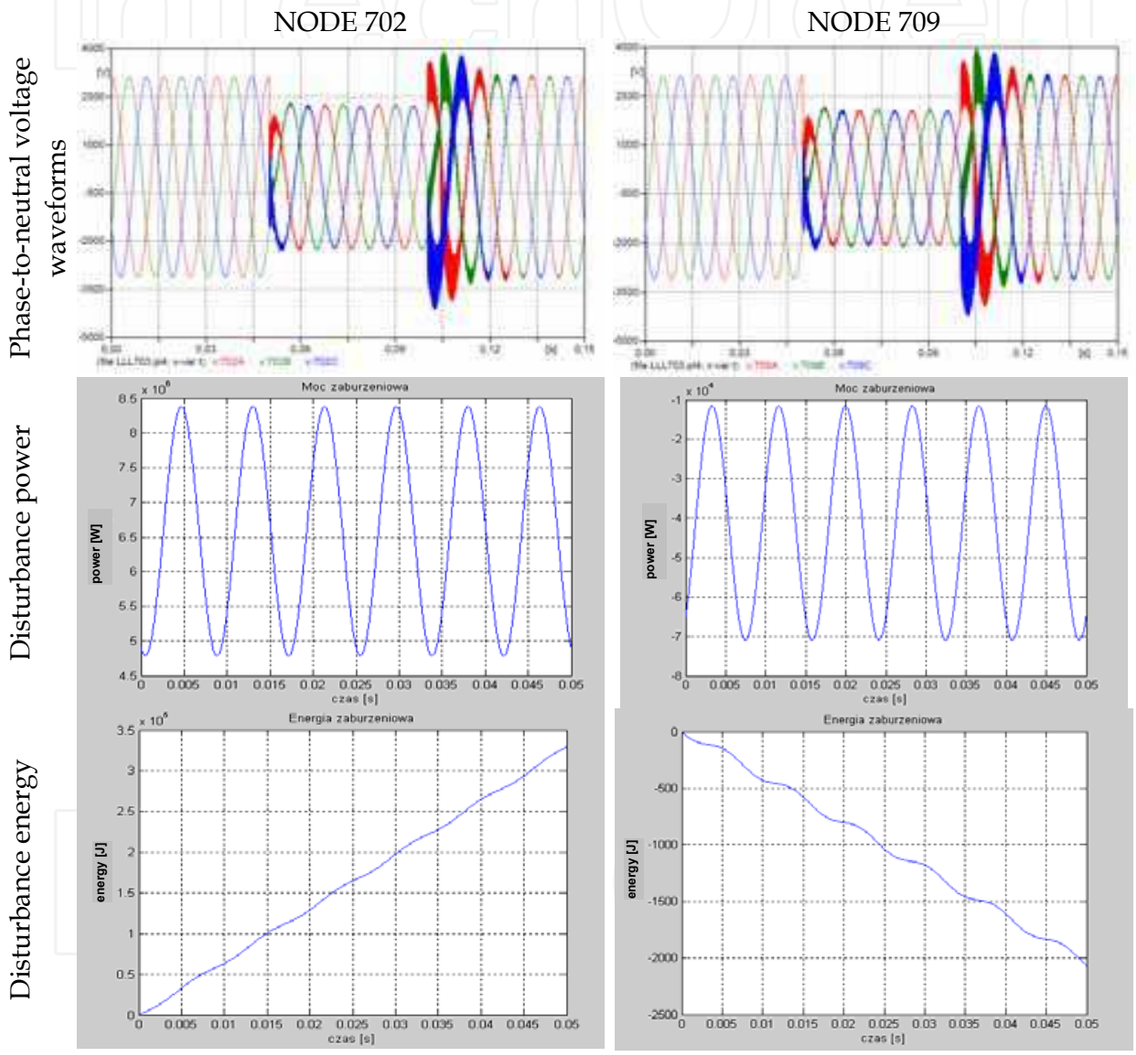


(b)

Fig. 19. The method of dip source location on the basis of the analysis of power and energy during the disturbance – example results of the simulation of a tree-phase short circuit in node 703 of the model network (Fig. 17a) waveforms of voltages and currents in nodes 702 and 709 as well as of disturbance power and energy

Fig. 19 shows the results of simulation studies aimed at locating the voltage dip source using the network model such as that in Fig. 17a. A three-phase short circuit, which occurred in

node 703, has been simulated; the study investigated if the disturbance in nodes 702 and 709 was located correctly. Correct conclusions are guaranteed also in the case of other types of short circuits.

### 3.5 Voltage criterion

In this method the dip source is located only on the basis of voltage measurement [20]. It consists in comparing the dip depth at the primary and secondary side of the transformer before and after the dip (Fig. 20):

$$U_1^* = \frac{U_{1-dip}}{U_{1-before}} \qquad U_2^* = \frac{U_{2-dip}}{U_{2-before}} \tag{35}$$

where $U_{i\text{-}dip}$ is the voltage during the dip, while $U_{i\text{-}before}$ is the voltage before the dip occurrence. The value by which voltage decreases on both sides of the transformer is represented by the following equations:

$$\Delta U_1 = Z_1 I_{SC} \qquad \Delta U_2 = (Z_1 + Z_{Tr}) I_{SC} \tag{36}$$

where $Z_{Tr}$ is the transformer impedance, and $I_{SC}$ is the short-circuit current. The value by which voltage decreases is higher at this side where the dip source is located. Therefore, if $\Delta U_2 > \Delta U_1$ ($U_2^* \rangle U_1^*$), the dip source is located at the lower side; otherwise, it is located at the upper side (orientation according to the direction of active power flow).

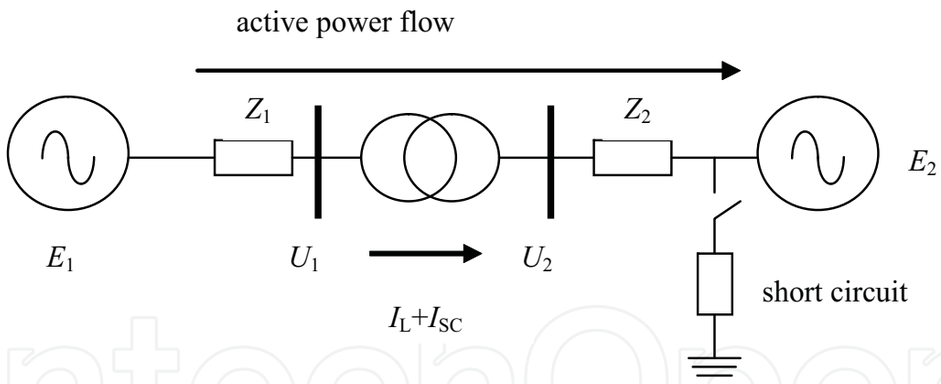


Fig. 20. The circuit showing the method of voltage dip location [20]

If the lower side of the system does not contain any energy sources and the dip source is located at the upper side, $U_1$ and $U_2$ have the same value in relative units.

The described method can easily be applied to transformers with connections of Y-Y type, which is a typical connection in the case of transmission grids. On the basis of characteristics of various types of voltage dips according to Bollen's classification [6,20] describes relationships between dip depths at both sides of the transformer with a Δ-Y connection.

The nature of load may affect the correctness of conclusions. The original assumption that only a short circuit at the lower side of the system may lead to the increase of current flowing through the transformer may be wrong in the case of a constant power load and transient response of milliseconds. In such a case, voltage reduction during the dip also leads to the increase of load current.

### 3.6 The criterion using asymmetry indicators

The method is based on the analysis of the factors of voltage and current asymmetry in PCC (Fig. 21). As far as most industrial loads (such as induction motors, rectifiers) are concerned, the current asymmetry factor is considerably higher than the voltage asymmetry factor in the case of an asymmetrical dip the source of which is located at the supplier's side. For example, induction motor impedance for a negative sequence component is very low; hence, even low voltage asymmetry will cause a high value of current negative sequence component (such a phenomenon will not occur in the case of synchronous machines).

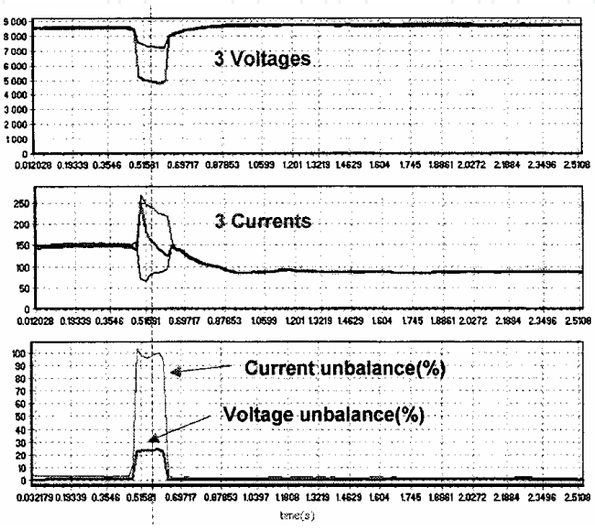


Fig. 21. Registration in PCC of an industrial consumer [39]

The disturbance source can also be located using the variation of phase angle $\Delta\Phi$ of the symmetric positive sequence component of current for the state before and during the short circuit [31]. The rule of the method is as follows: if $\Delta\Phi>0$, the dip is located "upstream" the PCC, otherwise it is located "downstream" the PCC, where the angle $\Delta\Phi$ is in the range $(-\pi) \div \pi$.

Drawing correct conclusions depends on the choice of period for the analysis before and after the short circuit occurrence in order to calculate the vector complex value of current symmetric component for both distinguished states.

### 3.7 The criterion of protection automatics systems functioning

Since voltage dips are mainly caused by short circuits, it is appropriate to use the knowledge of protection automatics systems in order to locate the dip source.

#### 3.7.1 The criterion based on the analysis of impedance variation

The concept of "increase impedance" applied in protection systems may be used as the basis for the dip source location [37]. It can be demonstrated that impedance calculated on the basis of current and voltage variations before and during the disturbance will be located in various quadrants of the complex plane, depending on the short circuit location. The procedure to follow is analogous to that presented in chapter 2.2, but this time it concerns the fundamental harmonic. The study is focused on the sign of the real part of the

impedance measured in PCC for the fundamental harmonic (according to the relationships presented in chapter 2.2). Since resistance should always have a positive sign, it is possible to locate the disturbance source on the basis of checking the sign of the real part of impedance $\underline{Z}_e$. Thus, the application algorithm of this method is as follows: equivalent impedance should be calculated in the measurement point during the registration of the disturbance in voltage, by means of the following equation:

$$\underline{Z}_e = \frac{\Delta \underline{U}}{\Delta \underline{I}} = \frac{\underline{U}_{dip} - \underline{U}_{before}}{\underline{I}_{dip} - \underline{I}_{before}} \tag{37}$$

where $(\underline{U}_{before}, \underline{I}_{before})$ and $(\underline{U}_{dip}, \underline{I}_{dip})$ are pairs of voltage and current fundamental harmonic values before and during the dip. The above method may be presented graphically on the complex variable plane. Since electrical power network impedance is usually of inductive character for the fundamental frequency, impedance $\underline{Z}_e$ vector will be most often located in the first or third quadrant of the coordinate system, like in Fig. 8. The conclusion algorithm is then as follows:

| | |
|---|---|
| If $Real(\underline{Z}_e) > 0$ | the source dip is located at the supplier's side |
| If $Real(\underline{Z}_e) < 0$ | the source dip is located at the consumer's side |

The above condition is true for current flow direction like in Fig. 2. In a practical algorithm it can be assumed that the current direction is compatible with the direction of active power flow.

This method can also be applied to asymmetrical voltage dips, due to the fact that the estimated value of impedance for the positive sequence component does not depend on the disturbance type.

In theory the method works correctly; there are, however, two basic difficulties in its application in practice.

The results (equivalent impedance values) are different for various voltage and current periods accepted for analysis before and during the dip. Accepting only one period as the basis for the analysis during the dip may give incorrect results. In order to improve the quality of conclusions drawn on the basis of this method the authors of [37] suggest a multi-period analysis and the method of least squares to estimate impedance or the choice of voltage period number on the basis of an additional analysis of power during the disturbance.

The **second** factor which may reduce the method reliability is the assumption concerning the linearity of the system. In fact, there are very often non-linear elements, i.e. regulated electric drives or induction motors at the consumer's side. Both types of the loads can operate with constant power. Their reaction during a voltage dip may be fundamentally different than that of linear loads. In order to reduce the influence of this factor some modifications of the investigated method are suggested [37].

Another impedance based methods is proposed in [30], which is based on the assumption that the estimated impedance during the voltage dip changes both in magnitude $|\underline{Z}|$ and in phase $\angle \underline{Z}$. Thus, new criterion is introduced, where the results obtained before and during the dip are compared, i.e.:

| | |
|---|---|
| If $\lvert\underline{Z}_{dip}\rvert\langle\lvert\underline{Z}_{before}\rvert$ and $\angle\underline{Z}$ >0 | the source dip is located at the supplier's side |
| Else | the source dip is located at the consumer's side |

### 3.7.2 The criterion using real current component

In order to locate the voltage dip source in relation to the measurement point the current active component measured in the measurement point is analysed; on the basis of its sign in the dip initial phase the disturbance source is located [16].
For a two-source system, the equivalent circuit diagram of which is presented in Fig. 22, the current flowing from source $E_1$ to $E_2$ is described by the following equation:

$$\underline{I} = \frac{\underline{E}_1 - \underline{E}_2}{\underline{Z}} \tag{38}$$

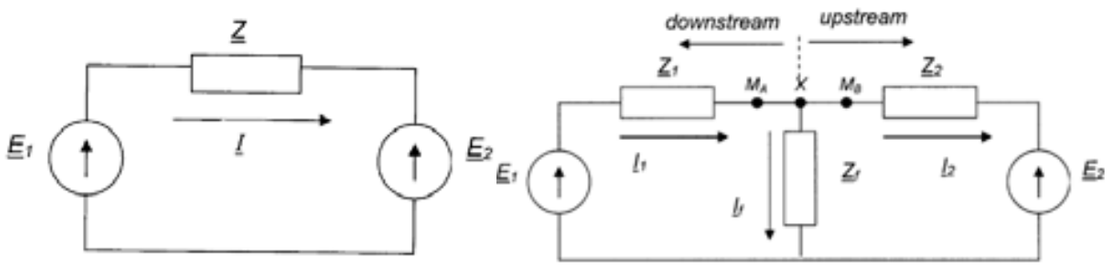


a) b)

Fig. 22. A two-source system: (a) before a short circuit; (b) during a short circuit [16]

Upon the short circuit in point X with short-circuit impedance $\underline{Z}_f$ , like in Fig. 22b, in point X voltage becomes reduced practically to 0. There are three currents in the circuit: $\underline{I}_1$ – flowing from the source $E_1$ , $\underline{I}_2$ – flowing from the source $E_2$ and $\underline{I}_f$ – flowing through the impedance $Z_f$. The direction of current $\underline{I}_1$ is the same as the direction of the current flowing before the short circuit occurred. If impedance $Z_2$ is much higher than impedance $Z_f$, current $I_2$ approximately equals zero, and the current of the source $E_1$ will be almost the only current flowing in the circuit. If the above condition is not satisfied, current $I$ is seen as the current flowing from the source $E_2$. This idea of the directions of currents during the short circuit is used for the voltage dip source location.
For a short circuit in point X voltage in point $M_A$ is:

$$\underline{U} = \underline{E}_1 - \underline{I}\underline{Z}_1 \tag{39}$$

where $\underline{U}$ and $\underline{I}$ are voltage and current measured in point $M_A$. Multiplying both sides of equation (39) by $\underline{I}^*$ results in the following equation:

$$\underline{U}\underline{I}^* = \underline{E}_1\underline{I}^* - I^2\underline{Z}_1 \tag{40}$$

The real part of equation (40):

$$UI\cos(\theta - \alpha) = E_1 I\cos(\phi_1 - \alpha) - I^2 R \tag{41}$$

where $\theta$ and $a$ are phase angles of, respectively, voltage and current in the measurement point $M_A$, while $\cos(\theta-a)$ is the power factor in point $M_A$.
On the basis of equation (41), in the measurement point $M_A$ the current flows from $E_1$ to X, and $I\cos(\theta-a)>0$. In such case it is concluded that the short circuit leading to the dip is located downstream the point $M_A$. In the case of the point $M_B$ the current $I\cos(\theta-a)<0$ is seen as the current flowing from $E_2$ to X, while the voltage dip source is located upstream the point $M_B$. The described method can also be applied to a single-source system.
If impedance $Z_f << Z_2$, the current from the source $E_2$ will not flow. However, in the initial phase of a voltage dip, the current resulting from a sudden change of circuit configuration can be considerably higher than the steady state current. Therefore, even if short-circuit impedance is very low, at the beginning of the short circuit a sudden change of the current direction can be observed. Consequently, the direction of current at the very beginning of the short circuit is a more appropriate indicator of the dip source location. So, the final procedure to follow in order to locate the dip source consists of the following steps: (i) measuring values and phase angles of voltage and current in the measurement point before and during the dip; (ii) determining the value of the component $I\cos(\theta-a)$ for a few periods before and during the dip; (iii) graphical representation of $I\cos(\theta-a)$ in the function of time and (iv) checking the sign of the component $I\cos(\theta-a)$ at the very beginning of the dip. If the sign is positive, the dip source is located at the lower side. On the other hand, if the sign is negative, the dip source is located at the upper side.

### 3.7.3 Criterion employing distance protection

Distance relays provide basic protection of HV electric power lines against all types of faults. The basis of their operation is measuring the impedance as "seen" from their terminals. Connection of all phase voltages and currents of the protected line to the relay analogue inputs, required for the correct impedance measurement, allows also determining fault location. This property of distance relays and their widespread application enable their use for voltage dips location [30].

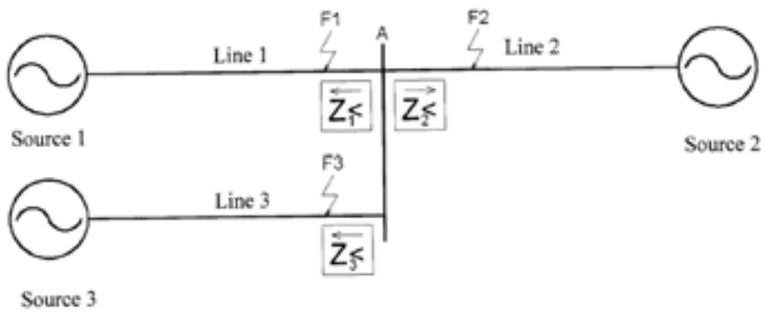


Fig. 23. A fragment of a power system

Fig. 23 shows busbars of substation A being a node of a power system. Each line bay at the substation is equipped with a distance relay "directed toward the line". It should be determined whether a voltage dip occurs "upstream" or "downstream" a specified point; it is assumed that this point is the bay of line 2. This information could be crucial for determining quality indices of power transmitted to or received from the second source. The subject of analysis are changes in the impedance($Z_2$<) seen by the distance protection of line 2 during faults $F_1$, $F_2$, $F_3$, that obviously will give rise to voltage dips at the above specified

measurement point. Upon the occurrence of fault $F_2$ a disturbance current will flow in the line 2 from the substation A busbars to the fault location. Thus the impedance seen by the distance protection $Z_2<$ decreases, and its phasor is situated in the first quadrant of complex plane. The occurrence of the faults at points $F_1$ or $F_3$ will cause in the line 2 a disturbance current flow towards busbars of the substation A. Therefore the impedance seen by the distance protection $Z_2<$ will also decrease, but its phasor will be situated in the third quadrant of a complex plane. The distance protection will select voltages and currents in proper phases in order to correctly determine the fault current loop impedance. Thus, the condition for a voltage dip occurrence upstream the protection, can be expressed as:

$$\left|Z_{dip}\right| < \left|Z_{before}\right| \; and \; \angle Z_{dip} > 0 \tag{42}$$

where:
$Z_{before}$ - the impedance seen by the distance protection prior to the fault occurrence,
$Z_{dip}$ – the impedance seen by the distance protection after the fault occurrence,
$\angle Z_{dip}$ – argument of the impedance as seen after the fault occurrence.
If the above condition is not fulfilled, but $\left|Z_{dip}\right| < \left|Z_{before}\right|$ then a fault, and consequently a voltage dip, is localized downstream the protection. It is also possible that the line 2 is disconnected due to a failure, maintenance or repair. In this case the occurrence of a fault at points $F_1$ or $F_3$ does not change the impedance seen by the protection at the measurement point. Thus this method does not prove itself for open networks and this is major disadvantage. A possible solution could be to combine the described algorithm with observation of the voltage at the measurement point. All newly installed distance relays are based on microprocessor technique and their structure contains under/over voltage protections. If the voltage at busbars decreases and a flow of short-circuit power from/toward busbars does not occur (the impedance seen by the directional protection does not change) we can infer that voltage dip occurs downstream the protection. Where the busbars voltage decreases, and the impedance seen by the directional protection changes, the algorithm described by relation (42) is employed.
Fig. 24 shows typical impedance characteristics of presently used directional protections. Most of protection zones are set in "forward" direction, usually only one zone is set in "reverse" direction. This results in a limited reach of correct location of voltage dips occurring downstream the protection since the reverse zone is set to a small distance. Another limitation for the use of distance relays is the method of their operation. They measure the impedance as seen from their terminals but the information about a change in the impedance is exclusively acquired by comparison with a threshold value. In other words, if the impedance does change but the change is not sufficient to exceed the threshold value, the protection will not detect it. A voltage dip caused by e.g. overloading the line 2 (Fig. 23) may cause a voltage reduction below the limit value but, because of insufficient sensitivity, the distance protection will not "recognize" the impedance change, leading thereby to erroneous location of the voltage dip. Also voltage dips of very short durations – below *20 ms*, may not be detected since the distance protection requires over *30 ms* for its proper operation. The above limitations result from the fact that distance protections are intended and designed for faults detection and clearing, and not for voltage dips detection.
Possible settings that would determine the information about a change in the impedance should be selected for the specific site at which this method is applied to voltage dips location.

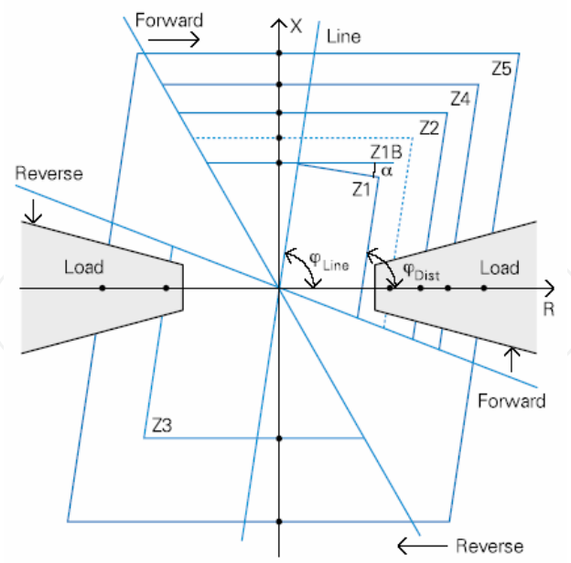


Fig. 24. Impedance characteristics of presently used directional relays

The advantage of the presented solution is its simplicity. The only procedure that should be carried out is a modification of the distance relay configuration, since all necessary electrical connections are already made during its installation.

In order to prove the above method and to illustrate its drawbacks were carried out simulation tests of the power system configuration shown in Fig. 23. The network voltage was assumed 110kV and lines lengths are as follows: line 1: 50 km; line 2: 10 km; line 3: 15 km.

The simulation was carried out for voltage dips caused by phase-to-earth and three-phase faults with transient resistance of the order of 1 Ω. The transient resistance values seen by distance protections, obtained for different locations of three-phase faults, are tabulated in tables 2-5. Results for phase-to-earth faults are not included because the obtained impedance values were, as expected, almost identical with those obtained for three-phase faults. Differences occurred solely in their real parts because of different values of phase-to-earth and three-phase fault currents and a non-zero transient resistance. Thus, without loosing generality of conclusions, the results for phase-to-earth faults can be disregarded.

Considering solely the protection *Z2*< it is evident from data in Table 2 that this protection identifies correctly voltage dips at busbars of substation A caused by faults in line 2 - the impedance module decreases and its phasor is situated in the first quadrant of complex plane. Such situation occurs even after disconnection of line 2 at its end. But if the line 2 is disconnected and a fault occurs at the point $F_3$, the impedance seen by *Z2*< does not change (Table 3). In this case the direction of a voltage dip can be inferred from the reduced busbars voltage and additional information that the line 2 is disconnected (the line current is zero).

Tables 3 and 4 show the impedance seen by the distance protections in the event of faults at the origin of lines 1 and 3. In both cases a decrease in the impedance *Z2*< is evident and its phasor is situated in the third quadrant of complex plane. Although the conditions of the method algorithm are fulfilled, a voltage dip at busbars of the substation A will be not correctly located. This is because the reverse zone pick up value shall be no greater than the impedance seen by this protection during a fault a the origin of line 3 (faults in lines 1 and 3 are located by the protection Z2< in its reverse zone). Thus voltage dips at the measurement point, caused by faults in line 1, will be correctly located exclusively in the case of faults near

to the substation A busbars. This results from significant differences in the lines lengths and may occur in real systems.

| No. of the distance protection | Impedance under normal operating conditions | | Impedance under disturbance conditions | |
|---|---|---|---|---|
| | module [Ω] | argument [deg] | module [Ω] | argument [deg] |
| Z1 | 262.1 | 298.0 | 12.7 | 210.2 |
| Z2 | 57.5 | 27.8 | 2.9 | 22.1 |
| Z3 | 53.4 | 194.5 | 3.8 | 200.4 |

Table 2. Fault in the middle of line (F2)

| No. of the distance protection | Impedance under normal operating conditions | | Impedance under disturbance conditions | |
|---|---|---|---|---|
| | module [Ω] | argument [deg] | module [Ω] | argument [deg] |
| Z1 | 183.7 | 347.1 | 48.2 | 192.6 |
| Z2 | ∞ | - | ∞ | - |
| Z3 | 183.5 | 167.4 | 48.2 | 12.9 |

Table 3. Fault at the origin of line 3 (F3) – line 2 disconnected

| No. of the distance protection | Impedance under normal operating conditions | | Impedance under disturbance conditions | |
|---|---|---|---|---|
| | module [Ω] | argument [deg] | module [Ω] | argument [deg] |
| Z1 | 262.1 | 298.0 | 13.8 | 48.5 |
| Z2 | 57.5 | 27.8 | 37.0 | 246.9 |
| Z3 | 53.4 | 194.5 | 22.0 | 214.7 |

Table 4. Fault at the origin of line 1 (F1)

| No. of the distance protection | Impedance under normal operating conditions | | Impedance under disturbance conditions | |
|---|---|---|---|---|
| | module [Ω] | argument [deg] | module [Ω] | argument [deg] |
| Z1 | 262.1 | 298.0 | 87 | 209.7 |
| Z2 | 57.5 | 27.8 | 25.3 | 184.1 |
| Z3 | 53.4 | 194.5 | 19.9 | 9.8 |

Table 5. Fault at the origin of line 3 (F3)

The method correctness depends to a large extent on the system configuration and this dependence results from the method of operation of the distance protection.

### 3.8 Vector-space approach [28]

The testing of all these methods show that in cases of asymmetrical voltage dips, they are rather ineffective. Furthermore, al the discussed methods, except the energy based one, require computation of voltage and current phasors for the fundamental-frequency component.

Because voltage dips are transient disturbance events, all phasor-based methods might produce questionable results due to inherent averaging in the harmonic analysis of the input signals [28].

<table>
<tr><th>Type of methods</th><th>Criterion</th><th>Notes</th></tr>
<tr><td>Voltage-current method</td><td>Slope $\left(\left\|\mathbf{u}_{\alpha\beta}(t)\right\|, S_{\alpha\beta}\left\|\mathbf{i}_{u,\alpha\beta}(t)\right\|\right)$<br>$>0 \rightarrow$ upstream<br>$<0 \rightarrow$ downstream</td><td> 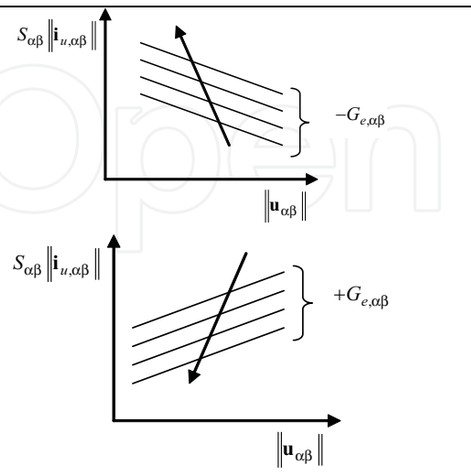
</td></tr>
<tr><td colspan="3">where:<br>$\boldsymbol{u}_{\alpha\beta}$ and $\boldsymbol{i}_{\alpha\beta}$ - voltage and current vectors defined in the orthogonal coordinate system αβ<br>$\left\|u_{\alpha\beta}(t)\right\|$ - norm of the voltage vector $\boldsymbol{u}_{\alpha\beta}$<br>$u_\alpha, u_\beta\left(i_\alpha, i_\beta\right)$ - components of vector $\boldsymbol{u}_{\alpha\beta}$ ($\boldsymbol{i}_{\alpha\beta}$) in the orthogonal coordinate system αβ<br>$p_{\alpha\beta}(t) = u_\alpha i_\alpha + u_\beta i_\beta$ - instantaneous real power [1]<br>$\boldsymbol{i}_{\alpha\beta}(t)=G_{e,\alpha\beta}\,\boldsymbol{u}_{\alpha\beta}(t)$<br>$G_{e,\alpha\beta}(t) = \frac{p_{\alpha\beta}(t)}{\left\|u_{\alpha\beta}(t)\right\|^2}$ $S_{\alpha\beta} = sign\left(G_{e,\alpha\beta}(t)\right)$ $S_{\alpha\beta}\left\|i_{u,\alpha\beta}(t)\right\| = \frac{p_{\alpha\beta}(t)}{\left\|u_{\alpha\beta}(t)\right\|}$</td></tr>
<tr><td>Active current based methods</td><td>If first peak of $S_{\alpha\beta} = sign\left(G_{e,\alpha\beta}(t)\right)$<br>$<0 \rightarrow$ upstream<br>$>0 \rightarrow$ downstream</td><td>Time response of $S_{\alpha\beta} = sign\left(G_{e,\alpha\beta}(t)\right)$ is calculated for a few cycles before and during voltage dips</td></tr>
<tr><td>Impedance based methods</td><td>If $\frac{sign\left(first\,peak\left(\Delta\left\|\mathbf{u}_{\alpha\beta}(t)\right\|\right)\right)}{sign\left(first\,peak\left(\Delta\left(S_{\alpha\beta}\left\|i_{\alpha\beta}(t)\right\|\right)\right)\right)}$<br>$>0 \rightarrow$ upstream<br>$<0 \rightarrow$ downstream</td><td>$\Delta\left\|u_{\alpha\beta}(t)\right\| = \left\|u_{\alpha\beta}(t)\right\|_{dip} - \left\|u_{\alpha\beta}(t)\right\|_{befor\,dip}$<br>$\Delta\left(S_{\alpha\beta}\left\|i_{u,\alpha\beta}(t)\right\| = \left(S_{\alpha\beta}\left\|i_{u,\alpha\beta}(t)\right\|\right)_{dip} - \left(S_{\alpha\beta}\left\|i_{u,\alpha\beta}(t)\right\|\right)_{before\,dip}\right)$</td></tr>
<tr><td>Energy based method</td><td>If $\Delta w_{\alpha\beta}(t) = \int_0^t \Delta p_{\alpha\beta}(\tau)\,d\tau$<br>$<0 \rightarrow$ upstream<br>$>0 \rightarrow$ downstream</td><td>$\Delta p_{\alpha\beta}(t) = p_{\alpha\beta}(t)_{dip} - p_{\alpha\beta}(t)_{before\,dip}$</td></tr>
</table>

Table 6. Voltage dip source detecting using vector space approach [28]

In order to overcome these difficulties vector-space approach is proposed for voltage dip detection. These methods are based on instantaneous voltage and current vectors and their transformation into α,β,0 Clarke's components. In this way other methods used for voltage dip source detection like the system operating conditions trajectory during the dip (chapter 3.2), the active current based method (chapter 3.7.2), impedance based methods (chapter 3.7.1) and energy based method (chapter 3.4) can be presented in general form.
In Table 6 are presented the generalized methods using a vector space approach.

## 4. Voltage flictuations

Voltage fluctuations are a series of rms voltage changes or a variation of the voltage envelope. Where only one dominant source of disturbance occurs its identification is usually a simple task. In extensive networks or in the case of several loads interaction, the location of a dominant disturbance source is a more complex process. Where large voltage fluctuations occur in several branch lines it may happen that measurements of flicker severity indices carried out at a power system node, do not indicate disturbing loads downstream the measurement point. The reason is a mutual compensation of voltage fluctuations from various sources.

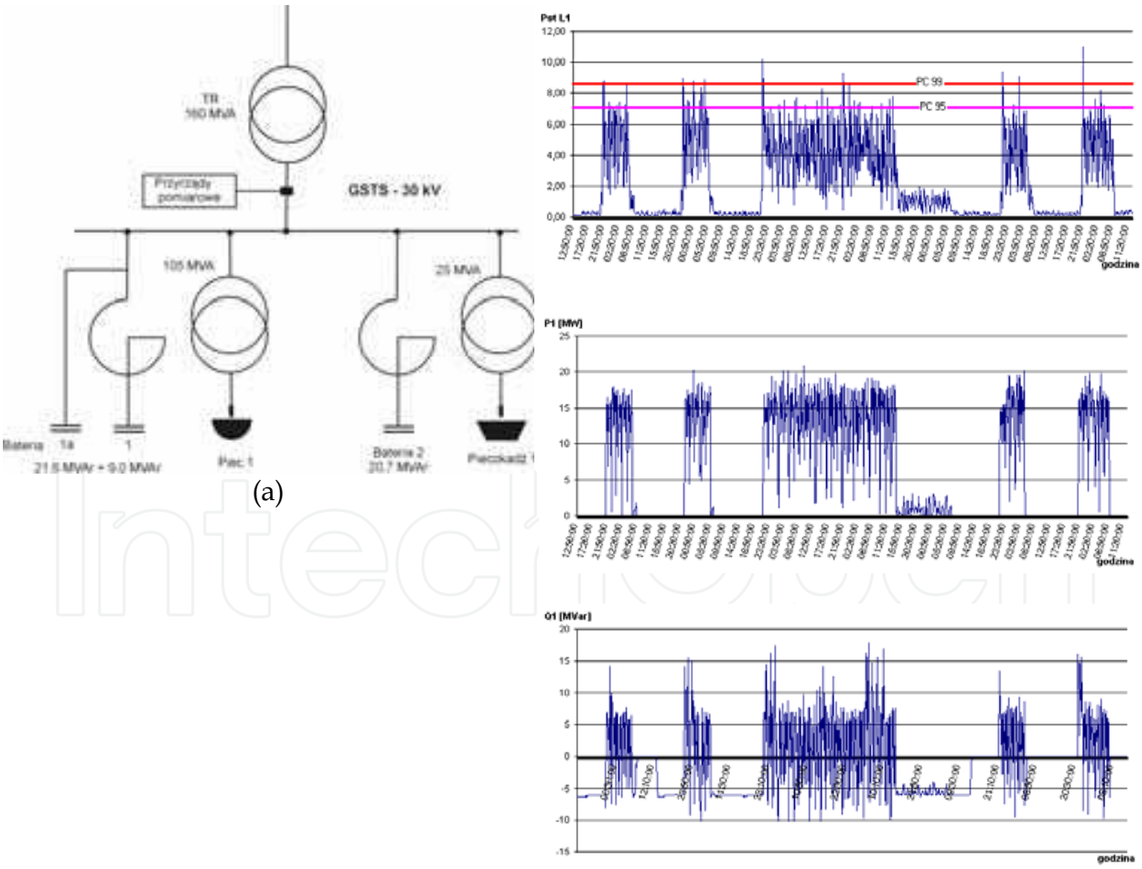


(a) (b)

Fig. 25. An example of changes in the flicker severity and the active and reactive power — phase L1 (diagram in (a))

### 4.1 Criterion of voltage fluctuations during a fluctuating load operation and after turning it off

The recorded quantities are: the flicker severity $P_{st}$ and changes in the reactive power $Q$ (also the active power $P$, if needed) at PCC. The measurements are carried out during the load operation and, where technically possible, after it is turned off. An example records from a steelwork during the arc furnace operation is shown in Fig. 25. Figure shows the results of one week's measurement of the flicker severity $P_{st}$, active power $P$ and reactive power $Q$ (phase L1). The dependence of flicker severity values on changes in power, caused by the arc furnace operation, is evident. During the periods the furnace is turned off the reactive power at the measurement point is capacitive due to the presence of fixed capacitor banks. In case several loads are analyzed the measurements have to be carried out during the operation of each load separately.

### 4.2 Correlation of changes in the flicker severity $P_{st}$ and/or changes in the active and reactive power

The method consists in the analysis of mutual correlation between changes in the reactive power $Q$ (and also the active power $P$, particularly for low-voltage networks) and the flicker severity value $P_{st}$. It allows define the dominant source of disturbance and assess the influence of a change in the load power on the voltage fluctuation in the measurement point. This method can also be applied for assessing the influence of disturbances in individual branches of the network on the total $P_{st}$ at PCC.

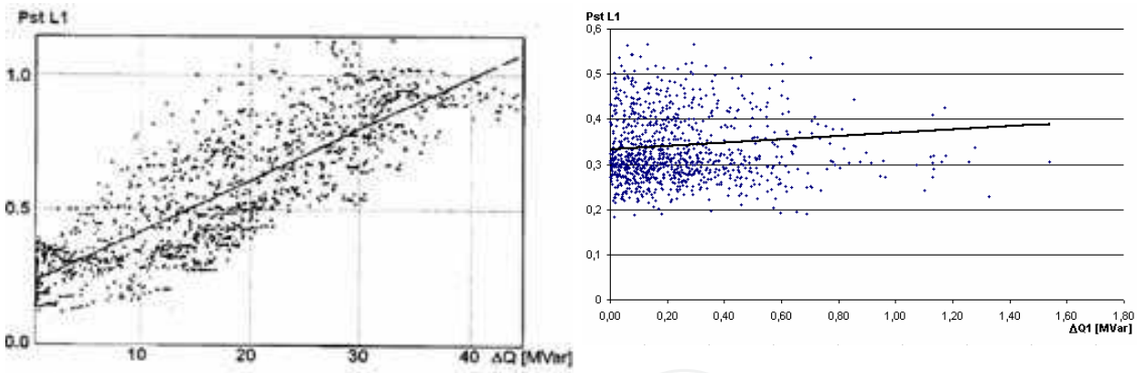


(a) (b)

Fig. 26. An example of correlation characteristics of flicker severity $P_{st}$ and reactive power changes

Fig. 26 shows correlation characteristics of flicker severity $P_{st}$ and reactive power changes. Characteristic (a) exhibits a strong correlation; it means that a load supplied from the monitored line is the dominant source of voltage fluctuation. In the case (b) the examined load cannot be regarded to be the dominant source.

### 4.3 Examination of the *U-I* characteristic slope [23]

Consider two sources of flicker which cause voltage fluctuation at the measurement location PCC: case 1 involves a flicker generating branch at point A and case 2 a similar at point B (Fig. 1). As a result of this flicker caused in the system, the voltage measured at PCC will fluctuate – the current at PCC will show different behaviour for these two cases, similar to criterion used for voltage dip localization.

For case 1, the measured current will be the load current at the lower voltage – the current measured at PCC will decrease as the voltage decreases during the flicker occurrence, and increase as the voltage increases (Fig. 27a).
For case 2, the measured current will be the sum of the load current and the flicker-caused load current at the lower voltage – therefore, the current measured at PCC will increase as the voltage decreases during the flicker occurrence, and decrease as the voltage increases (Fig. 27b).
These observations are presented graphically in Fig. 27. Each event is characterized by straight line, which represents the correlation between measured rms voltage and current. It can be seen that the slopes of the lines are different for the two cases. A positive slope shows that the flicker is from upstream and a negative slope shows that it is from downstream.
Although the idea was conceived for a one-source system, it has been found that it is also valid for two-source system as in Fig. 15 [23].

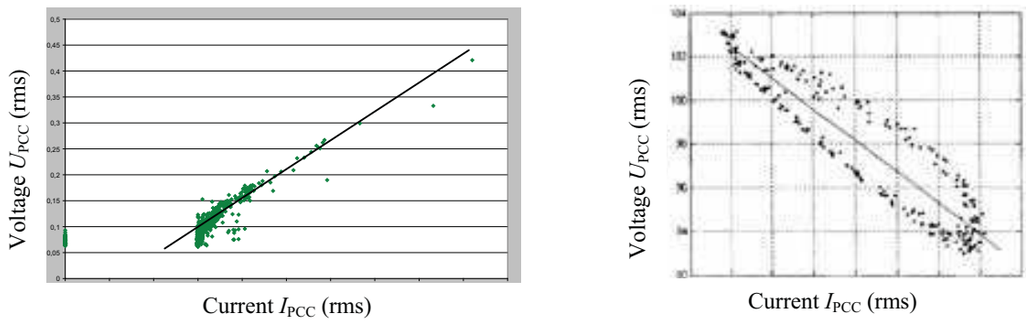


Fig. 27. Slope characteristics for the *U-I* correlations

### 4.4 Identification of interharmonic power direction [24]

The method utilises two common observations:

- interharmonics cause flicker – the fundamental and an interharmonic component of a voltage waveform are not in synchronous, therefore the voltage can be represented as the one of with modulated magnitude, which causes flicker.
- flicker cause interharmonics – voltage variations can be treated as amplitude modulation of the voltage, therefore by means of Fourier analysis the voltage can be decomposed on harmonic and interharmonic components.

Thus, the problem of locating flicker source can be solved by locating interharmonic source. If the customer appears as a source of interharmonics i.e. the active interharmonic power is negative, the customer is also a flicker source. If the customer appears as an interharmonic load i.e. the active interharmonic power is positive, the customer is not a flicker source.
The method is applied as follows:

- a power quality monitor is installed at the branch related to the suspected consumer, and records voltage and current waveforms as flicker occurs.
- Fourier based algorithm is used to investigate main interharmonics i.e. the components that have the maximum magnitude.
- for each of the interharmonic active power is calculated.
- if the consumer produces interharmonic power, he can be identified as interharmonic source and consequently the flicker source.

The frequency of an interharmonic signal depends on operation of the customer's equipment, so it is almost impossible that two devices produce the same interharmonics at the same time. Consequently it is relatively easy to locate the source of interharmonics. This method is fund not to be effective for random flicker source detection.

### 4.5 Examination of the "voltage fluctuation power"

A conception similar to the method of examining the direction of dominant interharmonics active power flow is presented in [1,3,4]. Similarly to the definition of active power in the time domain there could be introduced so called "flicker power". Lets define supply voltage and line current in PCC as sinusoidal waveforms with modulated amplitudes as follows

$$u_{PCC}(t) = \left(U_1 + m_U(t)\right)\cos\left(\omega_1 t\right) \qquad i_{PCC}(t) = \left(I_1 + m_I(t)\right)\cos\left(\omega_1 t + \varphi_I\right) \tag{43}$$

where $u_{PCC}(t)$, $i_{PCC}(t)$ are voltage and current waveforms respectively, $U_1$, $I_1$ are magnitudes of the fundamental components, $m_I$(t), $m_U(t)$ are amplitude modulation function of current and voltage respectively, $\varphi_I$ is phase shift of the current with respect to the voltage, $\omega_1$ is the angular frequency of the fundamental component.

The human sensitivity to flicker is a function of both modulating frequency and degree of modulation. That means the frequency signals $m_U(t)$ and $m_I(t)$ must be filtered according to how the human responds to flicker. This is achieved by using the sensitivity filter described in the IEC 61000-4-15. The out signals $m_{UF}(t)$ and $m_{IF}(t)$ indicate how an average human responds to flicker. By multiplying and integrating $m_{UF}(t)$ and $m_{IF}(t)$ a new quantity "flicker power" *FP* is achieved:

$$FP = \frac{1}{T}\int_0^T m_{UF}(t)m_{IF}(t)dt \tag{44}$$

where *T* is integration time. The flicker power provides two important pieces of information:

- the sign of *FP* provides information whether flicker source is placed upstream or downstream with respect to the monitoring point.
- when several consumers are investigated, magnitude of *FP* provides information which outgoing line contributes most to the actual flicker level.

Positive sign of flicker power means the same flow direction as the fundamental power flow. It means that voltage modulation $m_U(t)$ is correlated with current modulation $m_I(t)$ i.e. decreasing in supply voltage amplitude results in decreasing the load current. Consequently the flicker source is placed upstream with respect to the measuring point. Negative sign of flicker power means the opposite flow direction to the fundamental power flow, and consequently the voltage modulation is negative correlated with current modulation i.e. increasing the current load results in voltage drop. Therefore the flicker source is placed downstream with respect to the measuring point meaning that the load is responsible for voltage variation.

There could be noted, that the method is valid in a specific area of the load reactive power variation.

The method gives correct results under inductive load (the current lags the voltage), and limited capacitive power load (the current waveform leads the voltage waveform). There is also possibility of misinterpretation when a load of constant power demand is considered.

In such a case a voltage drop results in increased current flow. When the reaction is considerable it could be misinterpreted as having the flicker source downstream. The described situations, however, seldom arises in most practical situations.

## 5. Voltage asymmetry

A three-phase power system is called balanced or symmetrical if the three-phase voltages and currents have the same amplitudes and their phases are shifted by 120° with respect to each other. If either or both of these conditions are not fulfilled, the system is called unbalanced or asymmetrical.
The generator terminal voltages provided to the power system are almost perfectly sinusoidal in shape with equal magnitudes in the three phases and shifted by 120°. If the impedances of the system components are linear and equal for three phases, and if all loads are three-phase balanced, the voltages at any system bus will remain balanced. However, many loads are single-phase and some large unbalanced loads may be connected at higher voltage levels (e.g. traction systems, furnaces). The combined influence of such diverse loads, drawing different currents in each phase, may give rise to the 3-phase supply voltage unbalance. The supply voltage unbalance will then affect other customers connected to the same power network.
To quantify an unbalance in voltage or current of a three-phase system the symmetrical components (Fortescue components) can be used. The three-phase system is thus decomposed into a system of three symmetrical components: direct or positive-sequence, inverse or negative-sequence and homopolar or zero-sequence, indicated by subscripts 1, 2, 0. These transformations are energy-invariant, so for any power quantity computed from either the original or transformed values the same result is obtained. Thus, for active power of a three-phase system we obtain the equation:

$$P = P_s \tag{45}$$

where: $P = P_A + P_B + P_C = U_A I_A \cos\varphi_A + U_B I_B \cos\varphi_B + U_B I_B \cos\varphi_C$

and $P_s = 3(P_0 + P_1 + P_2) = 3(U_0 I_0 \cos\varphi_0 + U_1 I_1 \cos\varphi_1 + U_2 I_2 \cos\varphi_2)$

The subscripts A, B, C denote the different phases. It should be, however, noted that phase active powers have positive direction (from a source to load). Active powers of the symmetrical components $P_0, P_1, P_2$ have no physical meaning and their values depend on the character of the system asymmetry. It can be demonstrated that active power of the direct component has the same direction as the total system active power, but direction of active power of the inverse component depends on the system asymmetry nature. Direction of the inverse component may be used for identifying location of asymmetry source in the system.

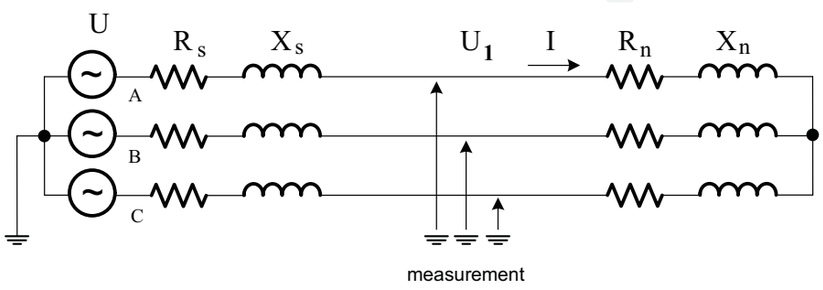


Fig. 28. Circuit diagram for asymmetry source location identification

| Circuit conditions | Active power components | | Source voltage | Measured voltage |
|---|---|---|---|---|
| | Load active power | Active powers of symmetrical components | | |
| Symmetrical | $P_{ABC} = 1060.5$ | $P_1 = 353.5$<br>$P_2 = 0$<br>$P_s = 3(P_{1s}+P_{2s}) = 1060.5$ | 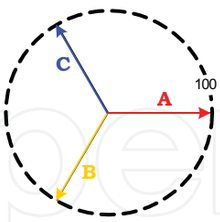 $U$ | 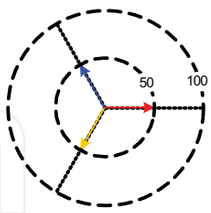 $U_1$<br> 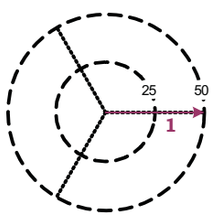 $U_{1s}$ |
| *Unbalanced load side parameters* (balanced system side parameters and phase voltages) | $P_{ABC} = 969.6$ | $P_1 = 352.2$<br>$P_2 = -29.0$<br>$P_s = 3(P_{1s}+P_{2s}) = 969.6$ | 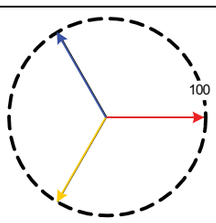 $U$ | 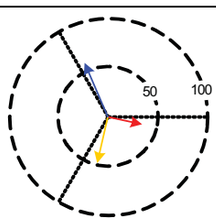 $U_1$<br> 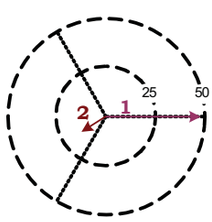 $U_{1s}$ |

Table 7. Comparative asymmetry analysis in the point of measurement

| | | | | |
|---|---|---|---|---|
| *Unbalanced system side parameters* (balanced load side parameters and phase voltages) | $P_{ABC} = 1280.4$ | $P_1 = 397.8$<br>$P_2 = 29.0$<br>$P_s = 3(P_{1s}+P_{2s}) = 1280.4$ |  | |
| *Unbalanced system phase voltages* (balanced system side parameters and load side parameters) | $P_{ABC} = 765.9$ | $P_1 = 245.5$<br>$P_2 = 9.8$<br>$P_s = 3(P_{1s}+P_{2s}) = 765.9$ |  | |

In order to examine the method of asymmetry source locating in the analysed diagram the following parameters are taken (in per unit values): $U$ = 100; $R_s$ = $R_n$ = $R$ = 3.536 and $X_s$ = $X_n$= $X$ = 3.536. Thus, for symmetrical conditions we obtain: $I$ = 10 and $U_1$ = 50.
The following sources of asymmetry in the circuit in Fig. 25 are considered:

- unbalanced load side parameters: $R_{nA} = 0.1R$, $R_{nB} = R$, $R_{nC} = 2R$,
  $X_{nA} = 0.1X$, $X_{nB} = X$, $X_{nC} = 2X$
- unbalanced system side parameters: $R_{sA} = 0.1R$, $R_{sB} = R$, $R_{sC} = 2R$,
  $X_{sA} = 0.1X$, $X_{sB} = X$, $X_{sC} = 2X$
- unbalanced system phase voltages: $\underline{U}_A = Ue^{j0^0}$ , $\underline{U}_B = 0,5Ue^{-j120^0}$ , $\underline{U}_C = Ue^{j120^0}$

Results of the calculation are shown in Table 7. As can be seen, the positive sign of the inverse component active power indicates the system side as the source of asymmetry at the point of measurement (irrespective to voltage or impedance asymmetry), the negative sign of the inverse component active power indicates the load side as the source of asymmetry.

## 6. Conclusion

In many cases, the quantitative determination of the supplier's and customer's share in the total disturbance level at the point of common coupling (PCC) is also required. Seeking non-expensive, reliable and unambiguous methods for locating disturbances and assessing their emission levels in power system, not employing complex instrumentation, is one of the main research areas which require the prompt solution. As a result, such research has become an important topic recently.

## 7. References

[1] Akagi H., Kanazawa Y., Nabae A.: Generalized theory of instantaneous reactive power in three-phase circuit, *Proceedings of the International Power Electronics Conference*, Tokyo, Japan, 1983, 1375-1386.

[2] Axelberg P.G.V., Bolen M., Gu L.: A measurement method for determining the direction of propagation of flicker and for tracing a flicker source, *International Conference CIRED'2005*, Turin (Italy), June 2005.

[3] Axelberg P.G.V., Bollen M.,: An algorithm for determining the direction to a flicker source, *IEEE Trans. on Power Delivery*, 21, 2, 755-760, 2006.

[4] Axelberg P.G.V., Bollen M., Gu L.: Trace of flicker sources using the quantity of flicker power, *IEEE Tran. On Power Delivery*, 23, 1, 465-471, 2008.

[5] D'Antona G., Muscas C., Sulis S.: Harmonic source estimation: a new approach for the localization of nonlinear loads, 978- 1-4244- 1 770-4/08, 2008 IEEE.

[6] Bollen M.H.J.: Understanding power quality problems – voltage sags and interruptions. *IEEE Press Series on Power Engineering* 2000.

[7] Chang G. W., Chen C. I, Teng Y. F.: An application of radial basis function neural network for harmonics detection, 978-1-4244-1770-4/08,2008 IEEE.

[8] Chen C., Liu X, Koval D.,, Xu W., Tayjasanant T.: Critical impedance method - a new detecting harmonic sources method in distribution systems, *IEEE Transactions on Power Delivery*, 19, 1, January 2004.

[9] Cristaldi L., Ferrero A.: Harmonic power flow analysis for the measurement of the electric power quality, *IEEE Tran. Instrum. Meas*, 44, 6,1995, pp. 683-685.

[10] Dán A.M.: Identification of flicker sources, *8th ICHQP '98, Athens*, Greece, Oct. 14-16, 1998.
[11] De Jaeger E.: Measurement of flicker transfer coefficient from HV to MV and LV systems. UIEPQ-9630.
[12] De Jaeger E.: Measurement and evaluation of the flicker emission level from a particular fluctuating load, *CIGRE/CIRED Joint Task Force* C4.109, Oct. 2007.
[13] De Jaeger E.: Disturbances emission levels assessment techniques (CIGRE/CIRED Joint Working Group C4-109).
[14] Emanuel A. E.: On the assessment of harmonic pollution, *IEEE Trans. on Power* Delivery, 10, 3, 1995.
[15] *Guide to quality of electrical supply for industrial installations*. Part 5: Flicker, UIEPQ 1999.
[16] Hamzah N., Mohamed A., Hussain A.: A new approach to locate the voltage sag source using real current component, *Electric Power Systems Research*, 2004, vol. 72, pp. 113-23.
[17] IEEE guide for protective relay applications to transmission lines, *IEEE Std.* C37.113, 1999.
[18] IEEE Power Engineering Society, Distribution System Analysis Subcommitee, *IEEE* 37 Node Test Feeder
[19] Khosrayi A., Melendez J., Colomer J.: A hybrid method for sag source location in power network, *9th International Conference, Electrical Power Quality and Utilization*, Barcelona, 9-lI, October 2007.
[20] Leborgne R.C., Olguin G., Bollen M.: The Influence of PQ-Monitor Connection on Voltage Dip Measurements, *In Proc. 4th Mediterranean IEEE Conference on Power Generation, Transmission, Distribution and Energy Conversion*, Cyprus, 2004.
[21] Li C., Xu W., Tayjasanant T.: A critical impedance based method for identifying harmonic sources, *IEEE Transaction on Power Delivery*, 19, 1, April 2004.
[22] Li, C., Tayjasanant, T., Xu W., Liu X.: A method for voltage sag source detection by investigating slope of the system trajectory, *IEEE Proceedings on Generation, Transmission & Distribution*, 150, 3, 2003 pp.367-372.
[23] Nassif A., Nino E., Xu W.: A V-I slope based method for flicker source detection, *Annual North American Power Symposium*, Edmonton (Canada), October 2005, 0-7803-9255-8/2005 IEEE.
[24] Nasif A., Zhang D., Xu W.: Flicker source identification by interharmonic power direction, *IEEE CCECE/CCGEI'2005 International Conference*, Saskatoon (Canada), May 2005, 0-7803-8886-0/2005 IEEE.
[25] Nunez V.B., Moliner X.B., Frigola J.M., Jaramillo S.H., Sanchez J., Castro M.: Two methods for voltage sag source location. *13th ICHQP 2008*, Australia.
[26] Parsons A. C., Grady W.M., Powers E.J., Soward J.C.: A direction finder for power quality disturbances based upon disturbance power and energy, *IEEE Trans. Power Delivery*, 2000, 15, 3, pp. 1081-1086.
[27] Pfajfar T., Blaźić B., Papić I.: Methods for estimating customer voltage harmonic emission levels, 978-1-4244-1 770-4/08 IEEE.
[28] Polajzer B., Stumberger G., Seme S., Dolinar D.: Generalization of methods for voltage sag-sag source detection using vector-space approach, *IEEE Trans. on IA*, 6,45,2009.
[29] Prakash K. S., Malik O. P., Hope G. S. Amplitude comparator based algorithm for directional comparison protection of transmission lines, *IEEE Trans. on Power Delivery*, 4, 4, 1989, pp. 2032-2041.

[30] Pradhan A.K. , Routray A.: Applying distance relay for voltage sag source detection, *IEEE Trans. on Power Delivery*, 20, 2005, pp. 529-31.
[31] Pradhan A.K, Routray A., Madhan S.: Fault direction estimation in radial distribution system using phase change in sequence current, *IEEE Tran. on Power Delivery*, 22, 2007, pp. 2065-2071.
[32] Pyzalski T., Wilkosz K.: Critical analysis of approaches to localization of harmonic generation, *Electrical Power Quality and Utilisation*, Cracow, Sep. 17-19, 2003.
[33] Pyzalski T., Wilkosz K.: New approach to localization of harmonic sources in a power system, *Electrical Power Quality and Utilisation*, Cracow, Sep. 17-19, 2003.
[34] Pyzalski T.: Localization of harmonic sources in a power system, Ph.D. dissertation, Wroclaw University of Technology, 2006.
[35] Review of methods for measurement and evaluation of the harmonic emission level from an individual distorting load, *CIGRE 36.05/CIRED 2 Joint WG* CCO2, 1998.
[36] Stade D. etc.: Simultaneous measurements for analysing the flicker dissipation in meshed HV power systems, *8th ICHQP*, Athens, Greece, Oct. 14-16, 1998.
[37] Tayjasanant, T., Li C., Xu W.: A resistance sign-based method for voltage sag source detection. *IEEE Tran. on Power Delivery* 20, 4, 2005, pp. 2554-2551.
[38] Technical specification, 1133A Power Sentinel™, Arbiter Systems.
[39] *The 12th ICHQP Tutorial*, Portugal, October 1, 2006.
[40] Tsukamoto M., Kouda I., Natsuda Y., Minowa Y., Nishimura S.: Advanced method to identify harmonics characteristic between utility grid and harmonic current sources, *8th ICHQP*, Athens, Greece, Oct. 14-16, 1998.
[41] Wilkosz K.: A generalized approach to localization of sources of harmonics in a power system, *13th ICHQP*, Australia, 2008.
[42] Xu W., Liu Y.: A method for determining customer and utility harmonic contributions at the point of common coupling, *IEEE Trans. on Power Delivery*, 15, 2, 2000.
[43] Xu W., Liu X., Liu Y.: An investigation on the validity of power direction method for harmonic source determination, *IEEE Trans. Power Delivery*, 18, 1, 2003, pp. 214-219

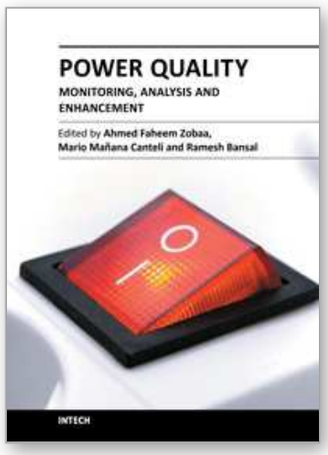


**Power Quality â€“Â Monitoring, Analysis and Enhancement**

Edited by Dr. Ahmed Zobaa

ISBN 978-953-307-330-9

Hard cover, 364 pages

**Publisher** InTech

**Published online** 22, September, 2011

**Published in print edition** September, 2011

This book on power quality written by experts from industries and academics from various counties will be of great benefit to professionals, engineers and researchers. This book covers various aspects of power quality monitoring, analysis and power quality enhancement in transmission and distribution systems. Some of the key features of books are as follows: Wavelet and PCA to Power Quality Disturbance Classification applying a RBF Network; Power Quality Monitoring in a System with Distributed and Renewable Energy Sources; Signal Processing Application of Power Quality Monitoring; Pre-processing Tools and Intelligent Techniques for Power Quality Analysis; Single-Point Methods for Location of Distortion, Unbalance, Voltage Fluctuation and Dips Sources in a Power System; S-transform Based Novel Indices for Power Quality Disturbances; Load Balancing in a Three-Phase Network by Reactive Power Compensation; Compensation of Reactive Power and Sag Voltage using Superconducting Magnetic Energy Storage; Optimal Location and Control of Flexible Three Phase Shunt FACTS to Enhance Power Quality in Unbalanced Electrical Network; Performance of Modification of a Three Phase Dynamic Voltage Restorer (DVR) for Voltage Quality Improvement in Distribution System; Voltage Sag Mitigation by Network Reconfiguration; Intelligent Techniques for Power Quality Enhancement in Distribution Systems.

**How to reference**

In order to correctly reference this scholarly work, feel free to copy and paste the following:

Zbigniew Hanzelka, Piotr Słupski, Krzysztof Piątek, Jurij Warecki and Maciej Zieliński (2011). Single-Point Methods for Location of Distortion, Unbalance, Voltage Fluctuation and Dips Sources in a Power System, Power Quality â€“Â Monitoring, Analysis and Enhancement, Dr. Ahmed Zobaa (Ed.), ISBN: 978-953-307-330-9, InTech, Available from: http://www.intechopen.com/books/power-quality-monitoring-analysis-and-enhancement/single-point-methods-for-location-of-distortion-unbalance-voltage-fluctuation-and-dips-sources-in-a-

INTECH
open science | open minds

**InTech Europe**
University Campus STeP Ri
Slavka Krautzeka 83/A
51000 Rijeka, Croatia
Phone: +385 (51) 770 447

**InTech China**
Unit 405, Office Block, Hotel Equatorial Shanghai
No.65, Yan An Road (West), Shanghai, 200040, China
中国上海市延安西路65号上海国际贵都大饭店办公楼405单元
Phone: +86-21-62489820

Fax: +385 (51) 686 166
www.intechopen.com

Fax: +86-21-62489821

IntechOpen